Chapter 7

Exploration of Solar Cosmic Ray Sources by Means of Particle Energy Spectra

Jorge Perez-Peraza and Juan C. Márquez-Adame

Additional information is available at the end of the chapter

http://dx.doi.org/10.5772/intechopen.77052

Abstract

Through the analysis of the energy spectrum of 12 ground level enhancements (GLE) of solar protons, a contribution in the understanding of the generation process of flare particles is attempted. Theoretical spectra of protons are derived by considering either they do not lose energy within the acceleration volume or that they are decelerated during the acceleration process. By comparing the theoretical source spectra with the experimental spectra, it is claimed that the generation process of solar particles develops under three main temperature regimes: the efficiency of particles acceleration is relatively high in cold-regimens decreasing while increasing the temperature of the medium. It is shown that in some events energy losses are able to modulate the acceleration spectrum within the source during the short time scale of the phenomenon, whereas in other events energy losses are completely negligible during the acceleration. It is argued that acceleration takes place in closed magnetic field lines and predicted the expansion and compression of the source material in association with the generation process of particles. This study allows us to estimate the range of variation from event to event of several parameters of the source and the acceleration process itself.

Keywords: solar protons, energy spectrum, solar sources, GLE

1. Introduction

Most of the information on solar flares has been generally supplied by the analysis of their electromagnetic spectrum; however, the confrontation of timing synchronization between

electromagnetic flare emissions with those of energetic particles and coronal mass ejections (CME) is the method utilized to explore the physical conditions and processes taking place in the sources of particle generation. For example, results obtained from the SEPS server project and future HESPERIA HORIZON 2020 project. However, the study of the corpuscular radiation emitted in some flares can also provide us with very valuable information about the physical conditions and processes occurring in association with this solar phenomenon. It is known, for instance, that the processes involved in the generation of solar particles are probably of a non-thermal nature, because the intensity of particles usually decays more softly than an exponential of a the thermal type does, and so other properties may be deduced in order to investigate how and where multi-GeV solar protons originate, that means the source parameters and the parameters involved in the generation process of particle [69, 70]. In this chapter, we attempt to draw some inferences concerning solar sources by the analysis of 12 ground level enhancements (GLE) of solar cycles 19 and 20.

It has been shown [40] that the best representation of the energy spectrum of solar protons through the whole energy domain explored experimentally at present is given by an inverse power law with an upper cutoff in its high energy portion. In fact, a good fit of the experimental data can be obtained with an exponential law in a limited energy band; however, a strong deflection is obtained with them as soon as a wider energy domain is involved. Besides, it has been established [11] that the measured differential intensity in solar proton events, as well as the source spectrum (inferred as an inverse power law in energy) are both velocity-dependent. Therefore, we infer that the acceleration rate of particles in the sun must provide the spectral shape and velocity dependence such as suggested by those results. This is the case with an energy gain rate of the form

$$\left(\frac{dW}{dt}\right)_{acc} = \alpha\beta W = \alpha\left(W^2 - \left(Mc^2\right)^2\right)^{1/2} \tag{1}$$

where β is the velocity of the particles in units of light velocity and W the total energy of particles. The parameter $\boldsymbol{\alpha}$ denotes the efficiency of the acceleration mechanism, which in the case of solar sources may be considered as roughly constant when the acceleration process reaches the steady-state in a given event [79, 80]. It has been generally thought that the energy loss processes of solar particles acceleration stage are not important in practice, and have only been taken into account after the acceleration stage in order to explain some features of electromagnetic emissions in solar flares and heating of the chromosphere [87].

In this chapter we shall consider, together with acceleration, energy loss processes occurring in the high density plasma of the solar source. It will be shown that energy losses in some proton flares can modulate the acceleration spectrum, thus implying that if such a small effect compared to the acceleration rate is able to modify the spectrum during the short lapse of the acceleration process, then the source spectrum is actually the result of a strong modulation due to local energy losses during acceleration and not only through interplanetary propagation; thus in Section 2, we discuss the basic equations of the more plausible energy loss processes in

particle sources. In Section 3, we present the observational energy spectrum of the concerned GLE as reported by several authors. In Section 4, we deduce theoretical source spectra, without and with energy losses during acceleration, disregarding energy changes of after acceleration while traversing the dense medium of the solar atmosphere to attain the interplanetary medium. In Section 5, we describe the criterion employed to construct integral energy spectra of solar proton (GLE) as well as the methods used in calculations; the results are presented graphically. In Section 6, the interpretation and significance of our results are discussed. In Section 7, the concluding remarks are summarized.

2. Energy losses of protons during acceleration in solar flares

Some researchers who study radiation and secondary particle fluxes consider an acceleration stage followed by a slowing down phase in the solar material once the action of the acceleration mechanism on particles has ceased (e.g. [86–89]); and they generally neglect the simultaneous occurrence of energy loss and acceleration.

However, particle acceleration is not performed in the vacuum but in the high density medium of flare regions; therefore, we shall study the local modulation of the acceleration spectrum as the protons are broken during the short-time scale of solar particle generation. The most important processes occurring in astrophysical plasmas capable of affecting the net energy change rate of particles in the range of kinetic energies of energetic solar protons ($E \sim 10^6$–10^{10} eV) are:

2.1. Collisional energy losses

These depend strongly on the density and temperature of the plasma; thus we assume that the main energy dissipation of particles must occur in the generation region, in the body of the flare itself. The rate of collisional losses in a medium of density $\boldsymbol{n}$ has been given in a simplified expression [37]

$$\left(\frac{dW}{dt}\right)_{ion} = -\frac{7.62 \times 10^{-9} nL}{\beta} \text{ (eV/sec)} \tag{2}$$

where $\beta = v/c$ is the particle velocity in terms of the light velocity, $\boldsymbol{L}$ is a unidimensional factor and logarithmically depending marginally on the particle energy. We shall assume a value of L $\sim$ 27 for solar flare conditions, when the medium concentration is $n \sim 10^{12}$ – 10^{13} cm^3. In **Figure 1**, the behavior of Eq. (2) with energy is shown. The complete description of collisional losses through the entire energy range including losses in the low energy portion (the so called nuclear stopping and electronic stopping) has been given by [10] for fully ionized hydrogen as:

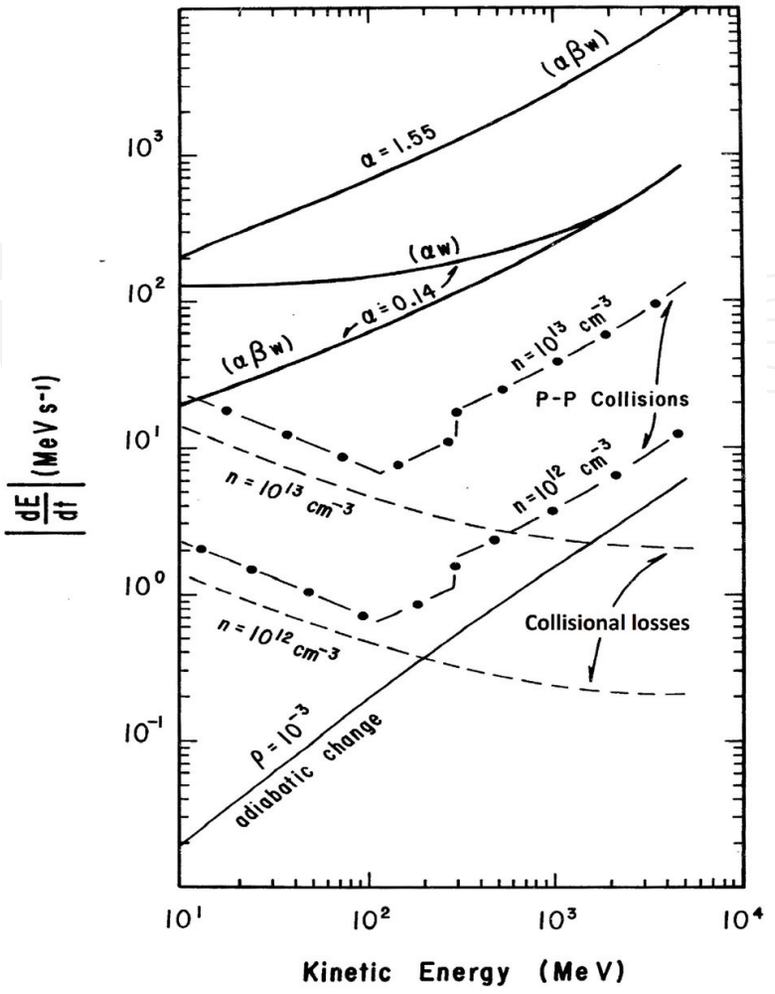

Figure 1. Energy change rates of protons (acceleration for two different rates) and deceleration for collisional losses p–p nuclear collisions and adiabatic cooling in a medium of density n = 10^{12}–10^{13} cm^{-3}.

$$\frac{dE}{dt} = -\frac{1.57 \times 10^{-35} N}{\beta} \frac{Q^2}{A} H(x) ln\Lambda \ \ (\text{eV/ns}) \tag{2.1}$$

where $x = 5.44 \times 10^4 \beta T^{-0.5}$, $H(x) = \xi_1 H_e(x_e) + \xi_2 H_p(x_p)$ with

$H_e(x_e) = 0.88 erf(x_e) - \left(1 - 5.48 \times 10^{-4}/A\right) x_e e^{-x_e^2}$ for electrons,

$H_p(x_p) = 0.88 erf(x_p) - \left(1 + \frac{1}{A}\right) x_p e^{-x_p^2}$ for protons,

$\xi_1 = 1.097803296 \times 10^{27}, \xi_2 = 5.979073244 \times 10^{23} and\ \Lambda = \left[4.47 \times 10^{16} A (T/N)^{0.5} \beta^2\right]/Q$

For the task of simplicity and because we are dealing in this work with GLE (high energy protons), we will use preferentially Eq. (2).

2.2. Energy degradation from proton-proton collisions

At present, there are evidences of the occurrence of nuclear reactions between solar nuclei and solar material, producing high energy gamma rays although is not absolutely clear whether nuclear reactions of solar energetic particles and solar material take place, when protons are injected into the photosphere, or they pass through coronal condensations, or during their acceleration within the dense material of flare regions. We shall assume that nuclear interactions occur at least in the acceleration volume where very likely the motion of energetic particles is completely random with respect to the local solar material. The isotropic motion of the accelerated particles is suggested by an analysis of neutron fluxes [45]. For purposes of energy loss calculations, we do not take into account collisions protons with other nuclear species, because the maximum energy change in elastic scattering occurs when the colliding particles have similar mass. Although the energy dissipation from *p: p* collisions is believed to appear mainly from elastic scattering, however at high energies (>750 MeV), the inelastic cross-section becomes highly important [44] increasing up to a maximum at some GeV, where it remains practically constant. In fact, as pion production initiates at $\sim$ 285 *MeV* and a fraction $\geq$ 35% of the kinetic energy of the incident proton goes into pion energy, then, energy dissipation from inelastic *p: p* scattering is not negligible in a high density medium ($\boldsymbol{n} \geq 10^{12}$ cm^{-3}). Concerning inelastic *p: p* interactions, the gamma ray line at 2.2 *MeV* due to fast neutron production, seems to be strong evidence of the occurrence of *p: p* collisions in solar flares. All this depends strongly on the production model: The assumed geometry and the spectral shape considered [2]. In fact, the cross-section for the later interactions is 10: 100 times higher, that is, their threshold is $\leq$36 *MeV/nucleon*, while that for inelastic *p: p* scattering are $\sim$ 285 MeV. Nevertheless, it has been known for a long time from [12] that solar abundances of CNO and he are of the order of $\sim$ 1.5: 7% with respect to the local *H*, in such a way that this kind of equilibrium between local abundances and interaction cross-sections states a high probability for the occurrence of *p: p* collisions in the body itself of the solar flare material. The main problem related with these features is that some reactions, as for instance $p(p; a\pi^0)p$ and multiple pion yielding at high energies, $p(p; a\pi^+)p$ or $p(p; a\pi^-, b\pi^0)p$ or $p(p;n, \pi^+, a\pi^+,a\pi^{--}, b\pi^0)$ by π^0 decay produce high energy solar gamma rays (50 *MeV*) that have neither been detected to our knowledge nor their plausible absorption into the solar material satisfactorily explained. In fact, the predicted wide peak for these gamma rays ranging from $\sim$38.5: 118 *MeV* [6] could probably render their identification difficult due to the presence of high energy photons expected from bremsstrahlung of very high energy solar electrons. In addition, there is the fact that high energy *p: p* reactions must occur more frequently, since the inelastic cross-section rises progressively from 290 *MeV* up to a maximum of about 1 *GeV* where it remains practically constant. Refs. [14, 15] have reviewed the problems connected with secondary products of nuclear interactions in solar flares. Nevertheless we show later in this work that *p: p* collisions are only expected in some few GLE. Hence, although the measured flux of particles does not distinguish whether solar protons have suffered nuclear collisions or not, the modulation of the energy spectrum by their effects furnish available information about their occurrence. The importance of energy degradation from *p: p* collisions in cosmic rays physics has been pointed out for the first time by [129]. The energy loss rate by nuclear interactions is agreement with [38]

$$\frac{dW}{dt} = -\sigma cn\beta W \ \ (\text{eV/sec}) \tag{3}$$

where σ in p–p collisions is composed of $\sigma_{p-p}^{ine} + \sigma_{p-p}^{el}$. As the inelastic cross-section is weakly energy dependent, it may be approximated to its mean value at high energies ($\sigma_{p-p}^{ine} \sim 26$ mb).· Concerning elastic collisions, a reasonable fit of the differential cross-section data by an analytical expression has been given by [91]. As the differential cross-section is highly isotropic, we can assume symmetry around 90°, such that their expression may be rewritten as $\sigma_{p-p}^{el} = hE^{-2} + JE^{-1}$ (if E ≤ 110 MeV) and $\sigma_{p-p}^{el} = hE^{-2}$ + f (if E > 110 MeV), where h = 96.09 mb-MeV^2, $j = 5.497 \times 10^3$ mb MeV and f = 46.49 mb. We have then from Eq. (3):

$$\left(\frac{dW}{dt}\right)_{p-p} = -cn\left(h\overline{E}^2 + j\overline{E}\right)\beta W \ (\text{if } E \leq 110 \text{ MeV})$$

$$\left(\frac{dW}{dt}\right)_{p-p} = -cn\left(h\overline{E}^2 + f\right)\beta W \ (\text{If } 110 < E < 290\ MeV)$$

$$\left(\frac{dW}{dt}\right)_{p-p} = -\left[\eta + cn\left(h\overline{E} + f\right)\right]\beta W \ \ (\text{If } E \geq 290 \text{ MeV}), \text{ where } \eta = cn\sigma_{in}$$

So that the net energy change can be compacted as:

$$\left(\frac{dW}{dt}\right)_{p-p} = -\left(hE^{-2} + jE^{-1} + f + \eta\right)\beta W \ \ (\text{eV/sec}) \tag{4}$$

where $h = 2.88 \times 10^{-15}$ n Me ^{2} s^{-1}, $j = 1.65 \times 10^{-13}$ n MeV s^{-1} *(if* $E \leq 110$ MeV*)*, $j = 0$ and $f = 1.39 \times 10^{-15}$ n s^{-1} *(if* $E > 110$ MeV*)*, $f = 0$ (*if* $E \leq 110$ MeV), $\eta = cn\sigma_{p-p}^{ine} = 8.1 \times 10^{-16}$ n s^{-1}, *(if* $E > 290$ MeV*)* and $\eta = 0$ *if* ($E < 290$ MeV). We have plotted Eq. (4) in **Figure 1** for two different values of the density n.

2.3. Adiabatic deceleration at the source level

Adiabatic cooling of cosmic particles in the solar wind has been proved long ago (e.g. [34]). However, here we are dealing with adiabatic cooling at the sources of solar energetic protons in GLE and not in the interplanetary or interstellar media medium. It is well-known that great flares are associated with magnetic arches, such as loop prominences and flare nimbuses (e.g. [7, 97, 98]) which occur between regions of opposite-polarity in the photosphere. Observations show that magnetic flux tubes expand from flare regions [23, 66, 107, 109, 117]. These configurations identified as "magnetic bottles" are usually related to the development of flare phenomena (e.g. [14, 83, 84, 96, 104, 110, 123]), therefore, we shall investigate the relationship between these magnetic structures and the phenomenon of particle generation through the study of the energy spectra of solar protons in GLE: We assume the hypothesis that particles are enclosed within those "magnetic bottles", where they are accelerated up to high energies.

Therefore, while the acceleration mechanism is in effect, and a fraction of particles are escaping from the flare region, the bulk of particles lose energy by adiabatic cooling due to the work that protons exert on the expanding material. Mechanisms for the expansion (or compression) of magnetic structures have been widely discussed (e.g. [96, 99]). It has been shown through energetic estimations that when particle kinetic density exceeds magnetic field pressure, the sunspot field lines are transported upward by the accelerated plasma; and thus, owing to the decrease of magnetic field density according to the altitude over the photosphere [1, 101], the magnetic bottles blow open at an altitude lower than 0.6: 1 R_s allowing particles] to escape into the interplanetary medium. Particles that have left the acceleration region before the magnetic bottle blows up may escape due to drift by following the field lines, or they remain stored therein losing energy losing energy until the magnetic structure is opened. We shall not consider this eventual deceleration during particle storage but only energy losses inside the acceleration volume. According to [46, 77], the energy change rate of particles by expansion (or compression) of magnetic fields producing adiabatic cooling or heating of the solar cosmic ray gas, when the non-radial components of the plasma velocity are negligible is given as

$$\left(\frac{dE}{dt}\right)_{ad} = \pm\frac{2}{3}\frac{V_r}{R}\mu E \ (\mathrm{eV/sec}) \tag{5}$$

where *Vr* and *R* are the velocity and distance of the plasma displacement, respectively, $\mu = 1 + \gamma^{-1}$ and $\gamma = W/Mc^2$. Hence, in terms of total energy *W* the adiabatic deceleration rate in the expanding magnetic fields may be expressed as

$$\left(\frac{dW}{dt}\right) = -\rho\beta^2 W \ (\mathrm{eV/sec}) \tag{6}$$

In order to estimate an approximate value for $\rho = (2/3)\ (V_r/R)$ in flare conditions, we extend the following considerations: it is known that the hydromagnetic velocity of the coronal expansion is in average of the order 400 km s^{-1}) and that in association with proton flares type IV sources systematically appear expanding with velocities in the range of 10^2–10^3 km s^{-1} depending on the direction of the expansion (e.g. [100, 101, 136]). Observations also show displacements with velocities of 650–2600 km s^{-1} in association with type II burst [95] and expansion of flare knots in limb flares with velocities in the range 5.3–110 km s^{-1} [54, 55, 83, 84]. Besides, it is also known that closed magnetic arches have a mean altitude of 0.6 *Rs* above the photosphere [122]. Therefore, assuming that the average velocity of 400 km s^{-1} is a typical value of magnetic motions in the chromosphere and low corona and an average expanded distance of the source of 0.3 R_s while acceleration is operating, we obtain thus $\rho \approx 10^{-3}$ s^{-1}. On the other hand, if we take into account the results usually associated with multi-Gev proton flares (GLE), then, magnetic loops expand $\sim$ 30,000 km with a velocity of $\sim$45 km s^{-1} at the time of the flare start, thus giving a value for ρ of the same order. We have illustrated Eq. (6) with $\rho = 10^{-3}$ s^{-1} in **Figure 1**.

It is expected that if the physical conditions in the source of multi-GeV solar proton flares and processes acting on solar particles must be similar, the behavior of the theoretical source spectra of solar protons from event to event will be similar, and thus by comparing the rates (1)–(6) the influence of each process on the acceleration spectrum can be established. For

instance, it can be seen from **Figure 1** that in the energy range 1–10^3 MeV and medium concentration $n = 10^{13}$ cm^{-3}, the ratio $r_1 = (dW/dt)_{p-p}/(dW/dt)_{coll}$ changes from r_1 = 1.7–16 and the ratio $r_2 = (dW/dt)_{ad}/(dW/dt)_{coll}$ varies from $r_2 = 4.6\ 10^{-5}$–0.64; therefore if all processes would act simultaneously in solar flares, the acceleration spectrum is mainly affected by energy degradation from *p–p* collisions, whose effects are stronger in the high energy portion of the spectrum. Collisional losses are more important in the non-relativistic region, whereas adiabatic losses become important in the relativistic region of the spectrum. Using experimental data of several GLE of solar protons, we shall investigate if the same processes occur in all events, and thus similar physical conditions are prevalent at the sources, or if they vary from event to event, in which, case it is interesting to investigate why and how they vary.

3. Experimental integral spectra of multi-GeV solar proton events

The description of the spectral distribution of solar particle fluxes of a given event is concerned, the result is a strong spread of spectral shape representations, according to the different detection methods employed, the energy bands and time intervals studied. The most plausible spectral shapes are described either by inverse power laws in kinetic energy or magnetic rigidity and exponential laws in magnetic rigidity (e.g. [53]). One of the most popular methods was developed by Forman et al, published in Ref. [59].

For example, in the case of the GLE of January 28, 1967, for which experimental measurements of fluxes through a wide energy range are available, several different spectral shapes have been analyzed: from the study of the relativistic portion of the spectrum, [60–62] proposes an exponential rigidity law $\{\sim exp.(-P/0.6\,(GV)\}$ and alternatively a differential power law spectrum in rigidity $(\sim P^{-5})$; [8] proposed a differential spectrum of the form $(\sim P^{-4.8})$ for relativistic protons of the event. Taking into consideration data from balloon, polar satellite and neutron monitors (N.M.), [3] gives an integral spectrum of the form $(\sim P^{-4})$; similarly, [40] deduced an integral spectrum as a power law in kinetic energy $(\sim E^{-2})$ with an upper cutoff at E_m = 4.3 GeV or in magnetic rigidity P as $(\sim P^{-3.1})$ with an upper cutoff at P_m = 5.3 GV. These authors have shown that as far as the whole energy spectrum through the different energy bands is concerned, any spectral shape that does not take into an upper cutoff is strongly deflected from the experimental data.

It would seem, therefore, that the description of energy spectra of solar particles is one of the most particular topics connected with solar cosmic ray physics: that is, owing to the lack of global measurements of the whole spectrum at a given time and to the lack of simultaneity in the measurements of differential fluxes, the integral spectra must be constructed with the inhomogeneous data available for each event. Therefore, in order to do so for 12 GLE during solar cycles 19 and 20, we have used low rigidity data (high latitude observations) for the following events: for September 3, 1960 event we have employed the 14:10 U.T. data from Rocket Observations [18] in the (0.1–0. 7) GV band. For November 12 and 15, 1960 GLE's, we have used the 18:40 U.T. and 05:00 U.T. data, respectively, from rocket observations in the (6.16–1.02) GV band [73]. For July 7, 1966 GLE, we have used the 19:06 U.T. data given by [57, 58] in the (0.13–0.19) GV band, and the spectrum given by [118] in the (0.19–0.44) GV band;

for higher rigidities (> 0.44 GV) we have employed the 03:00 U.T. measurements on Balloon and N.M. data given by [39]. In the events of November18, 1968, February 25, 1969, March 30, 1969, November 2, 1969 and September 1, 1971, we have used the peak flux data in the (0.1–0.7) GV band, given by [47] from the IMP4 and IMP5 satellite measurements. For January 24, 1971 GLE, we have employed the 06:05 flux data and at 07:20 U.T. in the (0.28–0.7) GV band from [134] For August 4, 1972 event, we have considered the HEOS2 graphical fluxes in the (0.15–0.45) GV band at 16:00 U.T. by [61] which lie between the 09:57–22:17 U.T. data of [4] and is in good agreement with N.M. measurements; for the (0.6–1.02) GV band we have employed the balloon extrapolated data by [61]. For the high rigidity portion of the spectrum (> 1.02 Gy), we have made use of the measurements given by [41–43] from NM data, in the following form:

$$J(>P) = K\int_{P}^{P_m} P^{-\Phi}dP \tag{7}$$

where K is a constant, P_m the high rigidity cutoff and Φ the spectral slope of the differential fluxes.

The values of P_m and Φ were taken through several hours around the peak flux of the event, as explained by the latter authors. The values of Φ were found to be systematically lower than other values furnished by GLE measurements due to the presence of the high rigidity cutoff parameter. For November 2, 1969 event we have taken the high rigidity power law spectrum as given by [61]; according to this data, we have considered a characteristic upper cutoff at 1.6 GV. In the case of August 4, 1972 event, we have taken the upper bound of Φ given for August 7 event by [43] considering that the particle spectrum became flatter with time during August 1972 events [4]. For the high rigidity cutoff, we have tested that within the error band, the value was essentially the same of that of August 7 event.

The extrapolation of the high rigidity power laws to the integral fluxes of the lower rigidity branches, has allowed us to determine *K* from Eq. (7) and thus to construct the high rigidity branches of the proton fluxes. By smoothing fluxes of both branches we have obtained the experimental integral spectra, which we have represented in the kinetic energy scale with solid lines through **Figures 2–4**. We have verified the good agreement of the high energy power law shape deduced in this manner, with the corresponding integral slope of the differential power law in kinetic energy $\int_E^{E_m} E^{-\Phi}dE$ reported in several works by (e.g. [41–43]). However, although it is systematically true that the best fit for the experimental points is given by such a power law, it is also true that there are some points that do not fit perfectly with that kind of curve; we have attempted to include these points in the experimental curves in the case of some GLE events. For January 28, 1967 event, we employed the integral spectrum deduced by [40] with the previously mentioned characteristics. It must be emphasized that the choice of these 12 multi-GeV proton events (GLE) follows from the fact that they furnish particle fluxes through a large range of energy bands and because of the information of the experimental value of E_m in these cases, which unlike the other parameters of the spectrum is the only one that does not vary through the propagation of particles into the interplanetary space as shown by [40]) and therefore, can be directly related to the acceleration process

An excellent review of solar cosmic ray events has been given in [130].

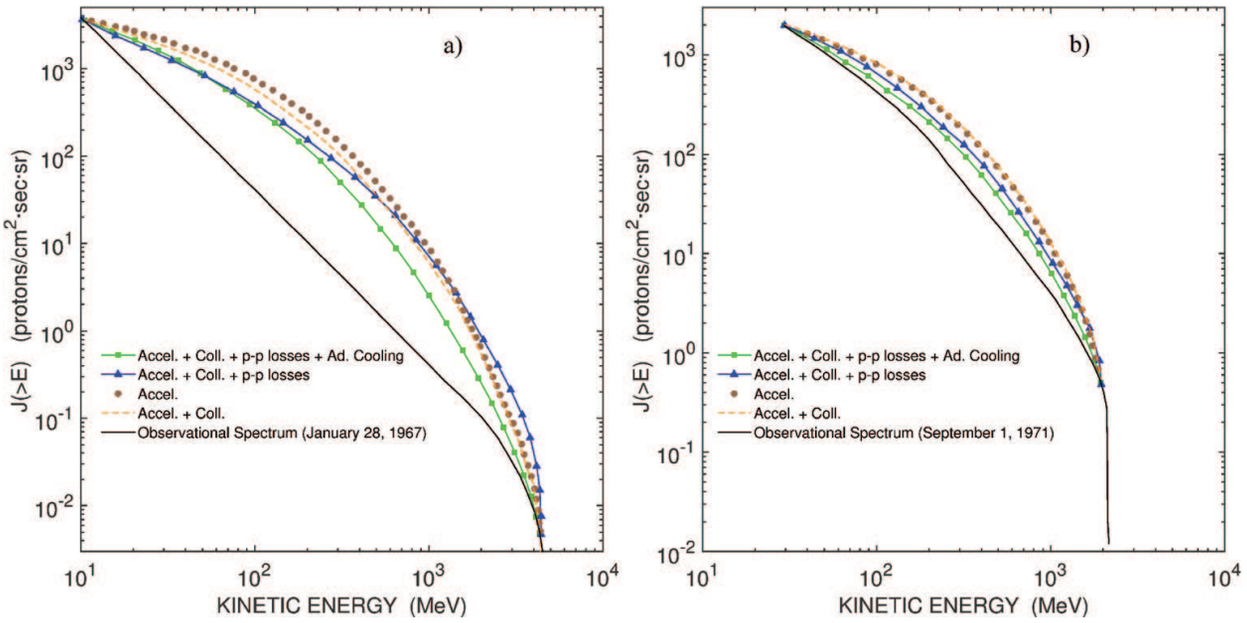

Figure 2. Theoretical and observational integral energy spectrum of *hot* events.

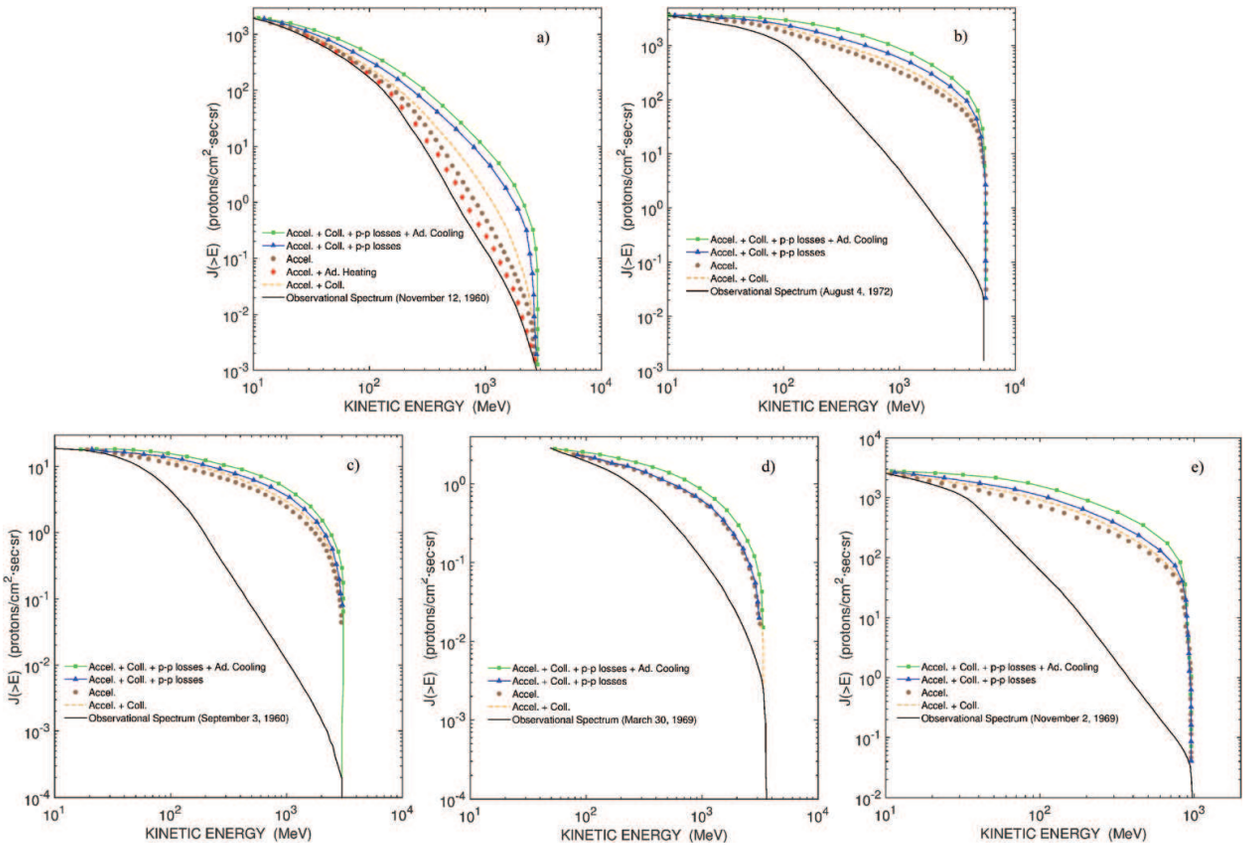

Figure 3. Theoretical and observational integral energy spectrum of *cold* events.

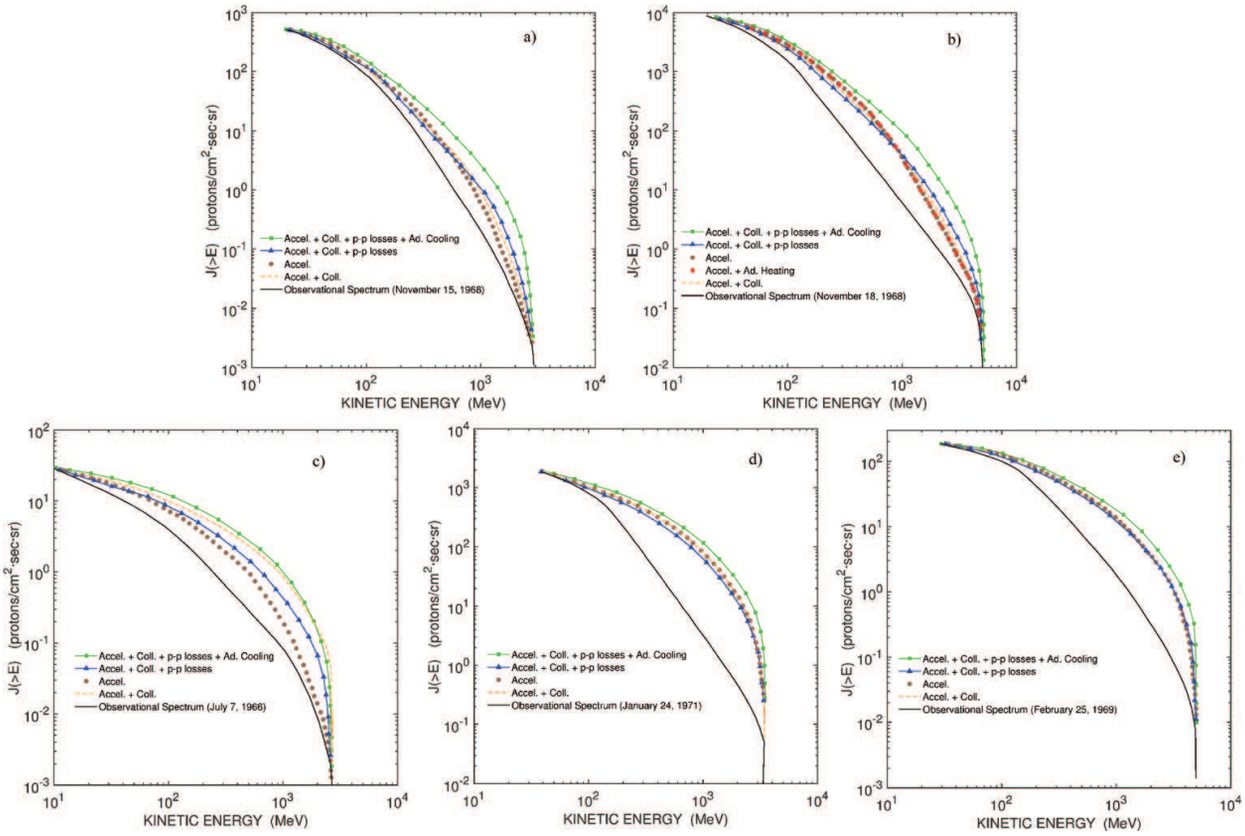

Figure 4. Theoretical and observational integral energy spectrum of *warm* events.

4. Theoretical spectra of solar protons in the source

In order to deduce the velocity and time dependent theoretical spectrum of the accelerated protons, one must take into account the various processes which affect particles during the remaining time within the acceleration volume. The main processes acting on particles during acceleration in a high density plasma are related either to catastrophic changes of particle density from the accelerated flux or to energy losses. Whereas the first kind of processes affect mainly the number density of the spectrum, energy losses entail a shift of the particle distribution toward lower energies, and a certain degradation of the number density due to thermalization of the less energetic particles. The number density changes on the accelerated proton flux may occur from catastrophic particle diffusion out of the flare source or by nuclear disintegration or creation of solar protons by nuclear reactions. Given the lack of knowledge about the exact magnetic field configuration and thus of the confinement efficiency of these fields, we do not consider here the effects of plausible escape mechanisms [26, 27, 104] on the theoretical spectrum. Therefore, to make a clear distinction between the energy loss effects (Section 2) on the spectrum of acceleration, we shall also neglect nuclear transformation during acceleration, local modulation post-acceleration and interplanetary modulation [67, 68] in this approach.

In addition, we shall not take into account spatial spread in the energy change rates within the acceleration process such that energy fluctuations [81, 82] which are considered minor for the purpose of this work.

It must be emphasized that since we are dealing with solar energetic particles, the well-known phenomena of Forbush decreases are rather related with galactic cosmic rays but not necessarily with solar energetic protons (e.g. [20]).

To establish the particle spectrum, we shall follow the assumptions that under the present simplified conditions lead to similar results that are obtained by solving a Fokker-Planck type transport equation on similar conditions [36, 81], that is, when the steady-state is reached in the source: we assume that a suprathermal flux with similar energy or a Maxwellian particle distribution is present in the region where the acceleration process is operating and a fraction $\boldsymbol{N_0}$ of them can be accelerated during the time interval in which the stochastic acceleration mechanism is acting [93]. The selection of particles follows to the fact that their energy must be ≥ than a critical energy, E_c, determined by the competition of acceleration and by local energy losses. By analogy with radioactive decay the energy distribution of cosmic ray particles is assumed as an exponential distribution in age of the form

$$N(E)dE = N(t)dt = \frac{N_0}{\tau}\exp\left(-t/\tau\right)dt \tag{8}$$

which in terms of the Lorentz factor is expressed as

$$N(\gamma)d\gamma = \left(1/Mc^2\right)N(t)\mathrm{dt} \tag{8.1}$$

where $\boldsymbol{t}$ is the necessary time to accelerate particles up to the energy E and $\boldsymbol{\tau}$ is considered as a mean confinement time of particles in the acceleration process. Eq. (8) represents hence the differential spectrum of the accelerated particles; to obtain the integral spectrum we take the integration of (8) up to the maximum energy of the accelerated protons, E_m (corresponding to the upper cutoff in the particle spectrum) the existence of which has been shown by [43] as discussed before.

$$J(>E) = \int_E^{E_m} N(E)dE = \int_t^{t_m} N(t)dt = N_0\int_t^{t_m}\frac{e^{-t/\tau}}{\tau}dt = N_0\left[e^{-t/\tau} - e^{-t_m/\tau}\right] \tag{9}$$

where t_m is the acceleration time up to the high energy cutoff. Because the acceleration process is competing with energy loss processes, the net energy gain rate is effectively fixed on particles, only beginning at a certain threshold value, E_c defined by $(dE/dt) = 0$, such that only particles with $E > E_c$ are able to participate in the acceleration process (the flux N_0). Thus the acceleration time $\boldsymbol{t}$ is defined as

$$t = \int_{E_c}^{E}\left(\frac{dE}{dt}\right)dt = t(E) - t(E_c) \tag{10}$$

Similarly the constant value t_m, representing the acceleration time up to the high energy cutoff, E_m defined as $t_m = t(E_m) - t(E_c)$, where $t(E_c)$ denotes the time of the acceleration onset. Therefore, Eq. (9) can be rewritten as

http://dx.doi.org/10.5772/intechopen.77052

$$J(>E) = N_0 e^{t(E_c)/\tau}\left[e^{-t(E)/\tau} - e^{-t(E_m)/\tau}\right] \tag{11}$$

4.1. The spectrum of acceleration

For the case in·which energy losses are completely unimportant within the acceleration time scale, the net energy change rate is determined by the acceleration rate, Eq.(1), which for simplicity's sake, we shall represent hereafter in terms of the Lorentz factor γ as

$$\left(\frac{d\gamma}{dt}\right) = \alpha\left(\gamma^2 - 1\right)^{1/2} \tag{12}$$

the condition $(d\gamma/dt) = (d\gamma/dt)_{acc} - (d\gamma/dt)_{loss} = 0$ gives $\gamma_c = 1$ (and hence $E_c = 0$), such that by integration of (12) we obtain the acceleration time up to the energy $E = Mc(\gamma - 1)$ as

$$t = \frac{1}{\alpha}\ln\left[\gamma + \left(\gamma^2 - 1\right)^{1/2}\right] \tag{13}$$

Now, by substitution of (13) in Eq. (8.1), we obtain the following differential spectrum

$$N(\gamma) = \frac{N_0}{\alpha\tau Mc^2}\left(\gamma^2 - 1\right)^{-1/2}\left[\gamma + \left(\gamma^2 + 1\right)^{1/2}\right]^{-1/\alpha\tau} \tag{14}$$

which in terms of total energy W is expressed as

$$N(W) = \frac{N_0}{\alpha\tau}\left(Mc^2\right)^{1/\alpha\tau}\frac{\left(1+\beta\right)^{-1/\alpha\tau}}{\beta}W^{-(1+1/\alpha\tau)} = \frac{N_0}{\alpha\tau}\left(Mc^2\right)^{1/\alpha\tau}\frac{\left\{W + \left(W^2 - \left(Mc^2\right)^{1/2}\right)\right\}^{1/\alpha\tau}}{\left(W^2 - \left(Mc^2\right)^2\right)^{1/2}} \tag{14.1}$$

When the parameter β is considered outside of the integrating equations a somewhat different expression is obtained:

$$N(W) = \frac{N_0}{\alpha\beta\tau}\left(Mc^2\right)^{1/\alpha\beta\tau}W^{-\left(1+1/\alpha\beta\tau\right)}$$

The corresponding integral spectrum of the accelerated particles appears from Eqs. (11)–(13) as

$$J(>E) = N_0\left[\left[\gamma + \left(\gamma^2 - 1\right)^{1/2}\right]^{-1/\alpha\tau} - \left[\gamma_m + \left(\gamma_m^2 - 1\right)^{1/2}\right]^{-1/\alpha\tau}\right] \tag{15}$$

(where) $\gamma_m = \left(E_m + Mc^2\right)/Mc^2$

the integral spectrum expressed in terms of kinetic energy becomes,

$$J(>E) = N_0\left(Mc^2\right)^{1/\alpha\tau}\left\{\left[E + Mc^2 + \sqrt{E^2 + 2Mc^2E}\right]^{-I/\alpha\tau} - \left[E_m + Mc^2 + \sqrt{E_m^2 + 2Mc^2E_m}\right]^{-I/\alpha\tau}\right\} \tag{15.1}$$

4.2. The modulated spectrum in the acceleration region

In order to study local modulation of spectrum (14) or (15) during acceleration, we shall proceed to consider energy loss processes together with the energy gain rate (12), according to the processes discussed in Section 2.

4.2.1. Modulation by collisional losses

When collisional losses are not negligible during acceleration, the net energy change rate is determined by (2) and (12) as

$$\frac{d\gamma}{dt} = \alpha\left(\gamma^2 - 1\right)^{1/2} - \left(b/Mc^2\right)\gamma\left(\gamma^2 - 1\right)^{-1/2} \tag{16}$$

where $b = 7.62 \times 10^{-9}$ nL, then, the solution of (16) is easily performed by employing a change of variable of the form $x = [(\gamma - 1)/(\gamma + 1)]$ [90], such that the acceleration time from the critical energy E_c up to the energy E, in terms of the Lorentz factor is

$$t = \ln\left|\frac{1+x}{1-x}\right|^{1/\alpha}\left|\frac{\phi^{1/2}x - (-Y_2)^{1/2}}{\phi^{1/2}x - (-Y_2)^{1/2}}\right|^{p} + \xi\tan^{-1}\left[x\left(\phi/Y_1\right)^{1/2}\right]\Big|_{x_c}^{x} = t(x) - t(x_c) \tag{17}$$

with $\varphi = b/Mc^2$, $Y_1 = 2\alpha + (4\alpha^2 + \varphi^2)^{1/2}$, $Y_2 = 2\alpha - (4\alpha^2 + \varphi^2)^{1/2}$, $p = Y_3/[2(-Y_2)^{1/2}\varphi^{1/2}]$, $Y_3 = (2\varphi/\alpha)[(\varphi\text{-}Y_2)/(Y_1\text{-}Y_2)]$, $Y_4 = (2\varphi/\alpha)[(Y_1\text{-}\varphi)/(Y_1\text{-}Y_2)]$, $\zeta = Y_4/(\varphi Y_1)^{1/2}$ and $x_c = [(\gamma_c\text{-}1)/(\gamma_c + 1)]^{1/2}$, where $\gamma_c = (b/2\alpha Mc^2) + 1$ is the critical value for acceleration determined by $(d\gamma/dt) = 0$, and the constant value $t(x_c)$ corresponds to the value of $t(E_c)$ appearing in Eq. (10). The differential spectrum of particles is obtained by substituting of (Eq. 17) in Eq. (8′) as follows

$$N(\gamma) = \frac{N_0}{\tau Mc^2}e^{t(x_c)/\tau}\frac{\left(\gamma^2 - 1\right)^{1/2}}{[\alpha(\gamma^2 - 1) - \phi\gamma]}\left(\frac{1+x}{1-x}\right)^{-1/\alpha\tau}\left[\frac{\phi^{1/2}x - (-Y_2)^{1/2}}{\phi^{1/2}x + (-Y_2)^{1/2}}\right]^{-\varnothing/2}\exp\left[(-q/\tau)\tan^{-1}\left[x\left(\phi/Y_1\right)^{1/2}\right]\right] \tag{18}$$

The integral spectrum is then from Eq. (11) and Eq. (17)

$$J(>E) = N_0\exp\left(t(x_c)/\tau\right)\left\{\left(\tfrac{1+x}{1-x}\right)^{-1/\alpha\tau}\left(\frac{\phi^{1/2}x - (Y_2)^{1/2}}{\phi^{1/2}x + (Y_2)^{1/2}}\right)^{-p/2}\exp\left[\left(-\frac{q}{\tau}\right)\tan^{-1}\left[x(\phi(Y_1)^{1/2}\right]\right]\right.$$
$$\left. - \exp\left(-t(x_m)/\tau\right)\right\} \tag{19}$$

where $t(x_m)$ corresponding to $t(E_m)$ in Eq. (11), appearing from the evaluation of Eq. (17) in the constant value $x_m = \left[\left(\gamma_m - 1\right)/\left(\gamma_m + 1\right)\right]^{1/2}$. It can be seen that spectra (18) or (19)reduces to (14) or (15) when b = 0. The integral spectrum in terms of kinetic energy is expressed as

$$J(>E) = N_0 \exp\left(\frac{t(E_i)}{\tau}\right)\left\{\left[\left|\frac{\varepsilon+E+Mc^2}{Mc^2}\right|^{-1/\alpha\tau}\left|\frac{(E-E_1)-\varepsilon+\left[E_1\left(E_1+2Mc^2\right)\right]^{\frac{1}{2}}}{(E-E_1)-\varepsilon-\left[E_1(E_1+2Mc^2)\right]^{\frac{1}{2}}}\right|^{-p}\right.\right.$$
$$\left.\left.\times\exp\left(\frac{-\left[E_2\left(-E_2-2Mc^2\right)\right]^{\frac{1}{2}}}{\alpha\tau(E_1-E_2)}\tan^{-1}\left(\frac{E\left(E_2+Mc^2\right)+Mc^2E_2}{\varepsilon E_2(-E_2-2Mc^2)}\right)\right)\right] - \exp\left(\frac{-t(E_m)}{\tau}\right)\right\} \quad (19.1)$$

with $p = \frac{\left[E_1\left(E_1+2Mc^2\right)\right]^{1/2}}{\alpha\tau(E_1-E_2)}$, $= \left(E^2+2Mc^2E\right)^{1/2}$, $E_i = b/2\ \alpha$ is the threshold value for effective acceleration and E_1, E_2 correspond respectively to $\left\{\left[b \pm \left(b^2+4\alpha^2\left(Mc^2\right)^2\right)^{1/2}\right]/2\alpha\right\}$. It can be seen that spectrum (19.1) reduces a spectrum (15.1) when $b = 0$.

The corresponding particle energy spectrum to Eq. (2′) is developed in the Appendix.

4.3. Modulation by proton-proton nuclear collisions

In the event that proton-proton collisions are important during the acceleration process. By adding Eq. (4), the net energy rate (16) turns into the following expression

$$\frac{d\gamma}{dt} = \alpha\left(\gamma^2-1\right)^{1/2} - \left(b/Mc^2\right)\gamma\left(\gamma^2-1\right)^{-1/2} - \left[h\left[Mc^2(\gamma-1)^{-2}+j\left[Mc^2(\gamma-1)\right]^{-1}+f+\eta\right]\right](\gamma-1)^{1/2} \quad (20)$$

The critical value γc for acceleration resulting when (dγ/dt) = 0 is obtained by solving a cubic equation of the form $A\gamma^3 + B\gamma^2 + C\gamma + D = 0$ with $A = \alpha(Mc^2)^2$, $B = -A-(b + j)Mc^2$, $C = -A + bMc^2-h$, $D = A + jMc^2-h$ if $E \leq 110$ MeV, or, $A = (\alpha-f)(Mc^2)^2$, $B = -A-bMc^2$, $C = -A + bMc^2-h$, $D = A-h$ if $110 < E \leq 290$ MeV and for the range $E > 290$ MeV similar to the last one but with $A = (\alpha-f-\eta)(Mc^2)^2$. Therefore, the roots a_1, a_2 and a_3 depend on α, b, h, j, f and η, such than when a medium concentration n is fixed, the basic dependence remains on α. Given that for the bulk of the involved parameters the conditions $a_1 > 1$, $a_2 \leq -1$ and $0 < a_3 \leq 1$ are systematically satisfied through all the energy ranges the relation $E_c = Mc^2\ (\gamma_c - 1)$ states a_1 as the critical value for effective acceleration. The acceleration time of particles beginning with this critical value up to the energy E is obtained from Eq. (20) as

$$t = \frac{1}{\lambda}\left\{\ln\left[\left|2\left(\gamma^2-1\right)^{1/2}+2\gamma\right|^{A_1a_1+A_2a_2+A_3a_3}\left|\frac{\gamma-a_1}{2\left(a_1^2-1\right)^{1/2}(\gamma^2-1)^{1/2}+2a_1\gamma-2}\right|^{A_1\left(a_1^2-1\right)^{1/2}}\right]\right.$$
$$\left. - \left[A_2\left(1-a_2^2\right)^{1/2}\sin^{-1}\left(\frac{a_2\gamma-1}{|\gamma-a_2|}\right)+A_3\left(1-a_3^2\right)^{1/2}\sin^{-1}\left(\frac{a_3\gamma-1}{|\gamma-a_3|}\right)\right]-t\left(\gamma_c\right)\right\} \quad (21)$$

where the constants. $A_1 = (a_1-1)(a_2-a_3)/\xi$, $A_2 = (a_2-1)(a_3-a_1)/\xi$ and $A_3 = (a_3-1)\ (a_1-a_2)/\xi$ emerge from the integration by partial fractions of Eq. (20), with $\xi = a_1^2(a_2-a_3) + a_2^2(a_3-a_1) + a_3^2(a_1-a_2)$, and take on different values according to the energy range concerned;

$\lambda = \alpha$ (if E ≤ 110 MeV), $\lambda = \alpha - f$ (if 110 < E ≤ 290 MeV) and $\lambda = \alpha - f - \eta$ (if E > 290 MeV). The differential spectrum in this case follows from Eqs. (8.1) and (20) as

$$N(\gamma) = \frac{N_0 Mc^2}{\tau} e^{t(\gamma_c)/\tau} \left|2\left(\gamma^2-1\right)^{1/2} + 2\gamma\right|^{-\delta} \left|\frac{\gamma - a_1}{2(a_1\gamma - 1) + 2\left(a_1^2-1\right)^{1/2}(\gamma^2-1)^{1/2}}\right|^{-\delta_1} \exp\left[-\delta_2 \sin^{-1}\left(\frac{a_2\gamma - 1}{|\gamma - a_2|}\right) - \delta_3 \sin^{-1}\left(\frac{a_3\gamma - 1}{|\gamma - a_3|}\right)\right] \frac{(\gamma-1)\left(\gamma^2-1\right)^{1/2}}{A\gamma^3 + B\gamma^2 + C\gamma + D} \tag{22}$$

where $\delta = (A_1a_1 + A_2a_2 + A_3a_3)/\lambda\tau$, $\delta_1 = A_1(a_1{}^2-1)^{1/2}\lambda\tau$, $\delta_2 = A_2(1 - a_2{}^2)^{1/22}/\lambda\tau$ and $\delta = A_3(1-a_3{}^2)^{1/2}/\lambda\tau$; therefore, the integral spectrum is given from (Eq. 11) and Eq. (21) as

$$J(>E) = N_0\left(Mc^2\right)^2 \left\{ e^{t(\gamma_c)/\tau} \left|2\left(\gamma^2-1\right)^{\frac{1}{2}} + 2\gamma\right|^{-\delta} \left|\frac{\gamma - a_1}{2(a_1\gamma-1)+2\left(a_1^2-1\right)^{\frac{1}{2}}(\gamma^2-1)^{\frac{1}{2}}}\right|^{-\delta_1} \times \exp\left[-\delta_2 \sin^{-1}\left(\frac{a_2\gamma - 1}{|\gamma - a_2|}\right) - \delta_3 \sin^{-1}\left(\frac{a_3\gamma - 1}{|\gamma - a_3|}\right)\right] exp\left[-t\left(\gamma_m\right)/\tau\right] \right\} \tag{23}$$

which in terms of kinetic energy becomes,

$$J(>E) = N_0 \exp\left(\frac{t(E_i)}{\tau}\right) \left\{ \left[\left|\frac{2}{Mc^2}\left[\left(E^2 + 2Mc^2E\right)^{1/2} + E + Mc^2\right]\right|^{-\delta_1} \left|\frac{2\left(a_1^2-1\right)\left(E^2+2Mc^2E\right)^{1/2} + 2a_1E + 2Mc^2(a_1-1)}{E + Mc^2(1-a_1)}\right|^{\delta_2} \cdot \left(\exp\left[A_2\left(1-a_2^2\right)^{1/2} \sin^{-1}\left(\frac{a_2E + (a_2-1)Mc^2}{|E+(1-a_2)Mc^2|}\right) + A_3\left(1-a_3^2\right)^{1/2} \sin^{-1}\left(\frac{a_3E+(a_3-1)Mc^2}{|E+(1-a_3)Mc^2|}\right)\right]\right)^{\delta_3} \right] - \exp\left(\frac{-t(E_m)}{\tau}\right) \right\} \tag{23.1}$$

where

$\delta_1 = \left[\left(Mc^2\right)^2/Q\tau\right](a_1A_1 + a_2A_2 + a_3A_3+)$, $\delta_2 = \left[\left(Mc^2\right)^2/Q\tau\right]A_1(a_2-1)^{1/2}$, $\delta_3 = \left(Mc^2\right)^2/Q\tau$

and Q, A_1, A_2, A_3, a_1, a_2, a_3, are constants that depend on α, b, η, h, j and f which emerge from the integration by partial fractions and take different values throughout the three different range considered.

4.4. Modulation by adiabatic processes

Under the consideration of adiabatic deceleration of protons while the acceleration mechanism is acting, the net energy change rate Eq. (20), is transformed by addition of Eq. (6) in

$$\frac{d\gamma}{dt} = \alpha\left(\gamma^2-1\right)^{1/2} - \left(Mc^2\right)\gamma\left(\gamma^2-1\right)^{-1/2} - \left\{h\left[Mc^2(\gamma-1)\right]^{-2} + j\left[Mc^2(\gamma-1)^{-1} + f + \eta\right]\right\} \times \left(\gamma^2-1\right)^{1/2} - \rho\left(\gamma^2-1\right)\gamma^{-1} \tag{24}$$

The condition $(d\gamma/dt) = 0$ for determining γ_c in this case, leads to a transcendental equation of the form $E\gamma^4 + F\gamma^3 + G\gamma^2 + H\gamma + I(\gamma-1)(\gamma^2-1)^{3/2} = 0$, whose solution depends only on $\boldsymbol{\alpha}$, $\boldsymbol{n}$ and

very weakly on ρ, and where $E = \alpha(Mc^2)^2$, $F = -E-(b + j)Mc^2$, $G = -E-h + bMc^2$, $H = E-h + jMc^2$ and $I = -\rho(Mc^2)^2$ in the range $E \leq 110$ MeV. Therefore, since critical energy for acceleration is defined in the low energy range, the wide interval $1.0 \leq \gamma \leq 1.1$ states a unique value of γ_c for any acceleration parameter α when the values of n and ρ are fixed. In order to deduce the particle spectrum, we have simplified Eq. (24) by changing variable $Z = \gamma-(\gamma^2-1)^{1/2}$, thus, obtaining in this way a rational function which integration by partial fractions gives the following acceleration time

$$t = \frac{1}{k}\left\{\left[ln\left(\left|z^2 + R_1z + R_2\right|^{c_{1/2}}\left|z^2 + R_3z + R_4\right|^{c_{3/2}}\left|z^2 + R_5z + R_6\right|^{c_{5/2}}\left|z^2 + R_7z + R_8\right|^{c_{7/2}} z^{c_9}\left|\frac{2z + R_1 - (\Delta_1)^{1/2}}{2z + R_1 + (\Delta_1)^{1/2}}\right|^{k_1}\right)\right.\right.$$
$$\left.\left. + k_2\, tan^{-1}\left(\frac{2z + R_3}{(-\Delta_2)^{1/2}}\right) + k_3\, tan^{-1}\left(\frac{2z + R_5}{(-\Delta_3)^{1/2}}\right) + k_4\, tan^{-1}\left(\frac{2z + R_7}{(-\Delta_4)^{1/2}}\right)\right] - t(z_c)\right\} \tag{25}$$

where $K_1 = (2C_2 - R_1C_1)/2\Delta_1^{1/2}$, $K_2 = (2C_4 - R_3C_3)/(-\Delta_2)^{1/2}$, $K_3 = (2C_6 - R_5C_5)/(-\Delta_3)^{1/2}K_1$

$K_4 = (2C_8 - R_7C_7)/(-\Delta_4)^{1/2}$; R_1, R_2, … R_8 are the coefficients of the quadratic factors Δ_1, Δ_2, Δ_3 and Δ_4 their discriminants, corresponding to two real and six complex roots of the nine roots of the rational function denominator, and C_1, C_2,. C_9 are the coefficients of the linear factors. For a given value of the acceleration efficiency $\boldsymbol{\alpha}$ all the quantities involved in (25) become constants and take on different values according to the three energy intervals studied. The factor κ is give as $\kappa = \alpha + \rho$ (if $E \leq 110$ MeV), $\kappa = \alpha-f-\eta$ (if $110 < E \leq 290$ MeV) and $\kappa = \alpha-f-\eta+\rho$ (if $E > 290$ MeV). As in the preceding cases, the substitution of Eq. (25) in (8′) furnishes us with a differential spectrum of the form

$$N(\gamma) = \frac{N_0}{Mc^2k\tau}e^{t(z_c)/\tau}\left(\frac{-z^8 + 2z^7 - 2z^5 + 2z^4 - 2z^3 + 2z - 1}{z^8 + Jz^7 + Mz^6 + Nz^5 + Pz^4 + Qz^3 + Rz^2 + Sz + V}\right)$$
$$\times\left\{\left(\left|z^2 + R_1z + R_2\right|^{-\theta_1}\left|z^2 + R_3z + R_4\right|^{-\theta_2}\left|z^2 + R_5z + R_6\right|^{-\theta_3}\left|z^2 + R_7z + R_8\right|^{-\theta_4}\right.\right.$$
$$\left.\left.\times\left|\frac{2z + R_1 - (\Delta_1)^{1/2}}{2z + R_1 + (\Delta_1)^{1/2}}\right|^{-\theta_5} z^{-\theta_6}\right) exp\left[\theta_7\, tan^{-1}\left(\frac{2z + R_3}{(-\Delta_2)^{1/2}}\right) + \theta_8\, tan^{-1}\left(\frac{2z + R_5}{(-\Delta_3)^{1/2}}\right) + \theta_9\, tan^{-1}\left(\frac{2z + R_7}{(-\Delta_4)^{1/2}}\right)\right]\right\} \tag{26}$$

$\Theta_1 = c_1/2\kappa\tau$, $\Theta_2 = c_3/2\kappa\tau$, $\Theta_3 = c_5/2\kappa\tau$, $\Theta_4 = c_7/2\kappa\tau$, $\Theta_5 = K_1/2\kappa\tau$, $\Theta_6 = c_9/2\kappa\tau$, $\Theta_7 = (-K_2)/\kappa\tau$, $\Theta_8 = (-K_3)/\kappa\tau$ *and* $\Theta_9 = (-K_4)/\kappa\tau$, $J = 2(F + I)/V$, $M = (4E + 4G + 2I)/V$, $N = (6F + 8H-GI)/V$, $P = (GE + 8G)/V$, $Q = (GP + 8H + GI)/V$, $R = (4E + 4c-2I)/I$, $S = 2\,(F-I)/V$, $V = (E + I)/V$ and $V = E-I$. The values of E, F, G, H, I in the range $E < 110$ MeV are the values given above; in the range $110 < E \leq 290$ MeV, E = $(\alpha-f)(Mc^2)^2$, F = E−bMc^2, G = −E + bMc^2, H = E−h and I = $\rho(Mc^2)^2$. In the range $E > 290$ MeV the only difference with the precedent range is $E = (\alpha-f-\eta)(Mc^2)^2$. The constant $t(Z_c)$ is the evaluation of (25) in the threshold value $Z_c = \gamma_c-(\gamma_c{}^2-1)^{1/2}$. The integral spectrum according Eq. (11) is,

$$J(>E) = N_0 e^{t(z_c)/\tau}\left\{\left(\left|z^2+R_1z+R_2\right|^{-\theta_1}\left|z^2+R_3z+R_4\right|^{-\theta_2}\left|z^2+R_5z+R_6\right|^{-\theta_3}\left|z^2+R_7z\right.\right.\right.$$
$$\left.+R_8\right|^{-\theta_4}\left|\frac{2z+R_1-(\Delta_1)^{1/2}}{2z+R_1+(\Delta_1)^{1/2}}\right|^{-\theta_5}\left|z^{-\theta_6}\right|\Bigg) exp\left[\theta_7\, tan^{-1}\left(\frac{2z+R_3}{(-\Delta_2)^{1/2}}\right)+\theta_8\, tan^{-1}\left(\frac{2z+R_5}{(-\Delta_3)^{1/2}}\right)\right. \quad (27)$$
$$\left.\left.+\theta_9\, tan^{-1}\left(\frac{2z+R_7}{(-\Delta_4)^{1/2}}\right)\right]-\exp\left(-t(z_m)/\tau\right)\right\}$$

where $t(Z_m)$ is the evaluation of Eq. (25) in $Z=\gamma_m-\left(\gamma_m^2-1\right)^{1/2}$ corresponding to the high energy cutoff value in the acceleration process.

In order to express the previous equation as a function of the kinetic energy E, the variable Z should be written as $Z(E)=\left(E+Mc^2\right)-\left(E^2+2EMc^2\right)^{1/2}$ and $Z(E)_m=\left(E_m+Mc^2\right)-\left(E_m^2+2E_mMc^2\right)^{1/2}$.

It is also interesting to analyze the opposite case, when instead of an expansion of the source materials, there is a compression of the source medium (e.g. [101–103]) with a consequent adiabatic acceleration of the flare particles, which entail a change of sign in the last term of the net energy change rate (24). Let us develop the situation for which energy losses are completely negligible in relation to the acceleration rate during the stochastic particle acceleration and compression of the local material

$$(d\gamma/dt)=\alpha\left(\gamma^2-1\right)^{-1/2}+\rho\left(\gamma^2-1\right)\gamma^{-1} \quad (28)$$

As in the case of Eq. (12) the threshold for acceleration is meaningless, and thus the acceleration time up to the energy E is given as

$$t=ln\left(\left|\frac{\gamma}{\alpha\gamma+\rho(\gamma^2-1)^{\frac{1}{2}}}\right|^{\chi}\left|\frac{\gamma+\left(\gamma^2-1\right)^{\frac{1}{2}}}{\gamma-(\gamma^2-1)^{\frac{1}{2}}}\right|^{\psi}\gamma^{\omega}|\alpha|^{\chi}\right) \quad (29)$$

where $=\frac{\rho}{(\alpha^2-\rho^2)}$, $\psi=\frac{\alpha}{2(\alpha^2-\rho^2)}$ *and* $\omega=\frac{\rho}{\rho^2-\alpha^2}$, consequently, the differential spectrum of particles is

$$N(\gamma)d\gamma=\frac{N_0}{mc^2\tau|\alpha|^{\chi/2}}\left|\frac{\gamma}{\alpha\gamma+\rho(\gamma^2-1)^{\frac{1}{2}}}\right|^{-\chi/\tau}\left|\frac{\gamma+\left(\gamma^2-1\right)^{\frac{1}{2}}}{\gamma-(\gamma^2-1)^{\frac{1}{2}}}\right|^{-\psi/\tau}\frac{\gamma^{(1-\omega/\tau)}d\gamma}{(\gamma^2-1)^{\frac{1}{2}}\left[\alpha\gamma+\rho(\gamma^2-1)^{\frac{1}{2}}\right]} \quad (30)$$

and then the integral spectrum is simply given as

$$J(>E)=\frac{N_0}{|\alpha|^{\chi/2}}\left(\left|\frac{\gamma}{\alpha\gamma+\rho(\gamma^2-1)^{\frac{1}{2}}}\right|^{-\chi/\tau}\left|\frac{\gamma+\left(\gamma^2-1\right)^{\frac{1}{2}}}{\gamma-(\gamma^2-1)^{\frac{1}{2}}}\right|^{-\psi/\tau}\gamma^{-\omega/\tau}-e^{-t\left(\gamma_m\right)/\tau}\right) \quad (31)$$

which in terms of kinetic energy becomes,

$$J(>E) = \frac{N_0}{|\alpha|^{\chi/2}} \left(\left| \frac{E + Mc^2}{\alpha(E + Mc^2) + \rho\left(E^2 + 2EMc^2\right)^{1/2}} \right|^{-\chi/\tau} \left| \frac{\left(E + Mc^2\right) + \left(E^2 + 2EMc^2\right)^{1/2}}{\left(E + Mc^2\right) - \left(E^2 + 2EMc^2\right)^{1/2}} \right|^{-\psi/\tau} \right.$$
$$\left. \left[\left(E + Mc^2\right)/Mc^2\right]^{-\omega/\tau} - e^{-t\left[\left(E_m + Mc^2\right)/Mc^2\right]/\tau} \right) \tag{31.1}$$

It is worth mentioning that although it is expected that the critical energy for acceleration E_c increases while adding energy loss process to the net energy charge rate, nevertheless, the value of E_c resulting from Eq. (24) is essentially the same as that obtained from Eq. (20). This can be understood from **Figure 1**, because adiabatic cooling is practically negligible at low energies.

5. Procedure and results

As seen in the preceding section, the calculation of our theoretical spectra, Eqs. (15),(19), (23), (27) and (31) requires three fundamental parameters, one of them directly related to the physical state of flare regions, that is, the medium concentration n, and the others concerning the acceleration mechanism itself, that is, the acceleration efficiency α and the mean confinement time τ. These last two depend of course on some of the physical parameters of the source, which we attempt to estimate from the appropriate values of α and τ. In the case of the solar source, we have considered the mean value of the electron density and a conservative value for the proton population as $n_e \approx n_H = 10^{13}$ cm^{-3} (e.g. [19, 35, 56, 113, 114, 116, 118]).

This assumption locates the acceleration region in chromospheric densities in agreement with some analysis of the charge spectrum of solar cosmic rays [64, 92].

Besides, since our expressions contain the acceleration parameter as the product $\alpha\tau$ and since we are dealing with particles of the same species, for the sake of simplicity we have adopted the assumption $\tau = 1{\cdot}s$ which allows us to separate the behavior of the acceleration efficient α in order to analyze it through several events and several source conditions. In any event, this value falls within the generally accepted range (e.g. [130, 131]); we shall discuss the implications of this assumption in the next section.

The determination of $\boldsymbol{\alpha}$ has been carried out through the following procedure: in order to represent the theoretical spectrum within the same scale as that of the experimental curve, we have normalized both fluxes at the minimum energy for which available experimental data are effectively trustworthy, in such a way as to state the maximum flux of particles at the normalization energy, E_{nor}

$$\left[J(>E)_{acc}\right]_{E_{nor}} = q\left[J(>E)_{earth}\right]_{E_{nor}} \tag{32}$$

where q is the normalization factor. Since our expressions do not directly furnish the source integral spectrum but rather $J(>E)/N_0$, we have deduced in this way a normalization flux K_0, keeping the same proportion with the differential flux N_0 appearing in our expressions

$$N_0 = qk_0 = protons/4\pi R_{SE}^2 s \quad (\text{protons/cm}^2\ \text{str}\ s) \tag{33}$$

where $R_{SE} = 1.5 \times 10^{13} cm$ = sun-earth distance. We have listed E_{nor} for every event on columns 8 of **Tables 1–3**.

The value of N_0 for every event is tabulated on columns 10 of **Tables 1–3**.

Assuming that the theoretical curve among Eqs. (15), (19), (23), (27) and (31) is near the experimental curve in a given event, describes the kind of phenomena occurring at the source better, we have proceeded to perform this intercomparison according to the following criterion: first, the condition stated by Eq. (32) at the normalization energy and, second, that $J(>E) \approx 0$ at the high energy cutoff E_m. In order to compare each one of the theoretical spectra with an

Hot Events		Specrum (31)	Spectum (15)	Specrum (19)	Specrum (23)	Specrum (27)	E_m (GeV)	E_n (MeV)	N_0(protons/cm^2 s str)
28/01/1967	$\alpha(s^{-1})$	0.18	0.18	0.19	0.23	0.21	4.30	10.00	2.1×10^{-12}
	E_c(MeV)	*****	*****	5.26	11.57	12.67			
01/09/1971	$\alpha(s^{-1})$	0.21	0.21	0.22	0.24	0.23	2.30	30.00	9.9×10^{-13}
	E_c(MeV)	*****	*****	4.54	11.09	11.57			

Table 1. Characteristic parameters of the acceleration process in solar protons ***hot*** events: acceleration efficiency α, high energy cutoff E_m, normalization energy E_n, flux of accelerated particles in the source N_0 and heliographic coordinates of the flare according to different reports.

Hot Events		Specrum (31)	Spectum (15)	Specrum (19)	Specrum (23)	Specrum (27)	E_m (GeV)	E_n (MeV)	N_0(protons/cm^2 s str MeV)
12/11/1960	$\alpha(s^{-1})$	0.13	0.14	0.17	0.26	0.26	2.600	15.000	3.891x10-11
	E_c(MeV)	15.32	14.30	13.45	9.67	10.58			
04/08/1972	$\alpha(s^{-1})$	0.59	0.60	0.70	0.90	0.93	4.280	15.000	1.979x10-11
	E_c(MeV)	4.28	4.21	3.87	3.06	2.97			
03/09/1960	$\alpha(s^{-1})$	0.72	0.73	0.83	0.98	0.99	2.960	10.000	4.704x10-16
	E_c(MeV)	2.96	2.92	2.77	2.40	2.39			
30/03/1969	$\alpha(s^{-1})$	0.91	0.92	0.95	0.99	1.08	2.340	50.000	1.449x10-15
	E_c(MeV)	2.34	1.18	2.42	2.38	2.48			
02/11/1969	$\alpha(s^{-1})$	1.54	1.55	1.76	2.10	2.59	0.915	10.000	2.342x10-11
	E_c(MeV)	0.84	0.84	0.81	0.66	1.05			

Table 2. Characteristic parameters of the acceleration process in solar protons ***cold*** events: acceleration efficiency α, high energy cutoff E_m, normalization energy E_n, flux of accelerated particles in the source N_0 and heliographic coordinates of the flare according to different reports.

Hot Events		Specrum (31)	Spectum (15)	Specrum (19)	Specrum (23)	Specrum (27)	E_m (GeV)	E_n (MeV)	N_o(protons/ cm^2 s str MeV)
15/11/1968	$\alpha(s^{-1})$	0.16	0.16	0.18	0.23	0.25	2.60	20.00	4.550x10-13
	E_c(MeV)	*****	*****	12.68	11.22	11.03			
18/11/1968	$\alpha(s^{-1})$	0.20	0.20	0.21	0.26	0.28	4.80	20.00	6.400x10-11
	E_c(MeV)	*****	*****	13.17	11.62	10.84			
07/07/1966	$\alpha(s^{-1})$	0.23	0.23	0.35	0.36	0.39	2.70	10.00	1.376x10-16
	E_c(MeV)	*****	*****	2.85	7.40	6.83			
24/01/1971	$\alpha(s^{-1})$	0.34	0.34	0.35	0.39	0.41	6.90	40.00	1.365x10-12
	E_c(MeV)	*****	*****	6.90	6.62	6.56			
25/02/1969	$\alpha(s^{-1})$	0.40	0.40	0.41	0.46	0.48	6.57	30.00	6.300x10-15
	E_c(MeV)	*****	*****	6.57	6.18	6.14			

Table 3. Characteristic parameters of the acceleration process in solar protons ***warm*** events: acceleration efficiency α, high energy cutoff E_m, normalization energy E_n, flux of accelerated particles in the source N_0 and heliographic coordinates of the flare according to different reports.

experimental curve under the same conditions, we could proceed to fix the value of the acceleration parameters in advance, which would entails making a priori inferences about the physical parameters of the source involved in the acceleration process of a given solar event; furthermore, this would result in a bias for the interpretation of the phenomenology involved in each event depending on the selected value of the efficiency α; that is, high values would give systematically the best fit with spectrum (27), whereas low values would show a systematically better fit with spectrum (15). Therefore, we proceeded conversely by determining the appropriate parameters of the source from the value of α in the theoretical spectra that best represents the experimental curve. The optimum values of α, obtained for each of the theoretical curves allows us to determine the critical energy E_c and the normalization flux K_o appropriate to each case. We have tabulated the values of α, E_c and K_o obtained for every event through calculations of the spectra (15) (19), (23), (27) and (31) in **Tables 1–3**. We have illustrated the optimum theoretical curves on **Figures 2–4**. From an examination of these results, it can be observed that no general conclusion can be drawn about the behavior of our theoretical spectra by the simple comparison of energy change rates (1), (2), (4) or (6) at different energy values 7 as if the medium density n were the only important parameter in determining the processes occurring at the source. Other factors must intervene, as can be seen from the fact that spectra behavior changes from event to event. Nevertheless, according to the behavior of particle spectra, we can group the solar events in three groups of similar characteristics: those illustrated in **Figure 2**, which we shall denominate *hot events*, where it can be seen that theoretical spectra progressively approach the experimental curves while adding energy loss processes to the acceleration rate. Therefore, the physical processes taking place at the source in those events are described by spectrum (27) indicating that adiabatic cooling of protons together with energy degradation from p–p collisions and collisional losses may have taken place. In this case spectrum (31) (illustrated only in the January 28, 1967 event) is systematically the more deflected curve, showing the absence of adiabatic compression, at least during the acceleration period. **Figure 3** shows the second group which we will call *cold events*, and

where it can be seen that energy losses are not important within the time scale of the acceleration process because theoretical curves get progressively separate from the experimental one while adding energy loss processes. Actually the best systematic approach in these cases is obtained with spectrum (31) (illustrated only for November 12, 1960 event) indicating that acceleration of protons by adiabatic compression could have taken took place. The third group that we shall distinguish as *warm* events is represented in **Figure 4**, where we can observe that there is no systematic tendency as compared to the previous groups. Nevertheless, it can be seen that at least at low energies the best approach to the experimental curve is described by spectrum (23), whereas at high energies the best fit is obtained with spectrum (15), thus indicating that to greater or lesser degree energy losses by collisional losses and proton-proton collisions may be important on low energy protons but they become negligible in relation to the acceleration rate in high energy particles. The point where this change may occur varies from very low energies in some events (July 7, 1966) to very high energies in others (January 24, 1971). The larger deflection from the experimental curve in these cases is obtained with spectrum (27), indicating that adiabatic expansion do not take place; furthermore, the fact that spectrum (31) (illustrated only for the November 18, 1968 event) is systematically deflected in relation to the acceleration spectrum (15) indicates that there is no adiabatic compression either. The values of the parameters describing the most adequate theoretical spectrum of events of **Figures 2–4** are tabulated on columns 7, 3 and 6 of **Tables 1–3**, respectively.

In order to estimate the amount of local plasma particles that must be picked up by the acceleration process to produce the observed spectrum, are must know the value of N_o in (8) when t = 0. Therefore, roughly assuming that at least for events of (**Figure 3**, **Table 2**), the picked up protons originate in a thermal plasma where the velocities distribution is of a Maxwellian-type, or that they appear from a preliminary heating related to turbulent thermal motions, then, it can be inferred that the primary differential flux is given as, related with the flux defined in Eq. (33).

$$N_0 = \left[9/(2\pi)^{3/2}\right](k/M)^{1/2}e^{3/2}nT^{1/2} \tag{34}$$

where M is the mass of protons and k the of Boltzman's constant. Then, by assuming that K_o is related to the flux of protons involved in the acceleration process and the flux N_o related to the original concentration of the medium, we have estimated from Eq. (33) the fraction of the local plasma particles that were accelerated in each event and tabulated them on columns 10 of **Tables 1–3**. In evaluating (34), we have assumed a different value of temperature T for each one of the 3 groups of events, before discussing them in the next section.

Now let us summarize the results which emerge from **Figures 2–4** and **Tables 1–3**, before extending their interpretation in next section:

1. The events illustrated in **Figure 2**, show the following features:

   i. In September 1, 1971 event, the best fit of the experimental spectrum is obtained with (27) whereas the worst fit is given by (15) and (31).

ii. The January 28, 1967 event follows the same tendency as the preceding event up to ∼800 MeV, with an exception at very low energies (≤ 30 MeV) where it can be seen that spectrum (23) is slightly better than (27). Beyond ∼800 MeV spectrum (23) becomes the more deflected curve. The low particle energy flux tail is noticeably similar to the minimum theoretical energy for effective acceleration ($E_c \sim 12$ MeV).

2. The events of **Figure 3** show that:

The best fit of the experimental curve is systematically given by spectrum (31) and (15) (e.g. the November 12, 1960 event), whereas spectrum (27) is systematically the most deflected one.

3. The events of **Figure 4** show the following characteristics

a. The theoretical curve which best approximates the experimental one at low energies is spectrum (23) followed by spectrum (19).
b. At given energy (from ∼500 to ∼3000 MeV) the previous tendency is abandoned, such that spectrum (15) interchanges sequential order with spectrum (23).
c. Spectrum (27) is systematically the most deflected curve at all energies.
d. Spectrum (31) is systematically deflected in relation to spectrum (15) (e.g. November 18, 1968 event).
e. The July 7, 1966 event, however, by following the feature (a) at E ≤ 25 MeV, beyond this energy spectrum (15) comes nearer to the experimental curve than spectrum (23), whereas spectrum (19) through a progressive, separation becomes the most deflected curve beyond ∼2000 MeV.

4. Examination of **Tables 1–3** shows the following features:

a. For a given event the obtained value of acceleration efficiency α is the same with spectrum (31) and (15) (columns 3 and 4 of **Tables 1** and **3**) contrary to the events of **Table 2**, in which case α is lower with spectrum (31) than with (15).
b. Examination of a given spectrum (same column 5, or, 6 or 7) shows that α and E_c behave in an inversely proportional manner.
c. For a given event, the values of α in the events of **Tables 2** and **3** (columns 4, 5, 6, and 7) increase monotonically while adding energy loss processes to the acceleration rate, with the exception of the events of **Table 1**, in which case the obtained values of α with spectrum (27) decrease in relation to the value of α from spectrum (23).
d. For a given event of **Table 1**, the value of E_c increases monotonically with the addition of an energy loss process to the net energy change rate, whereas in the events of **Tables 2** and **3** the value of E_c obtained from (27) (column 7) decreases in relation to the values obtained from spectrum (23).
e. The obtained value of K_0, (column 10) is related only to the magnitude of the event (i.e. the value of $J(>E)$ at E_n).
f. There is no correlation between E_m and the other parameters of the tables α, E_c, K_0, or heliographic coordinate; neither is there any correlation between the maximum flux at E_n and α or E_c.

g. If we ignore the fact that the assumed heliographic position of the flare associated to the January 28, 1967 event is relatively uncertain, it can be noted that there is a south asymmetry in the what we designate as *hot events* (**Table 1**), a north asymmetry in *cold* and *warm events* (**Table 2**) and a certain west and north asymmetry among the events of **Table 3**.

h. The critical energy E_c from *cold* and *warm* events is correlated with the temperature of the source in the sense that their values increase from *cold* to *warm* and from *warm* to *hot* events. The significance of the association of the parameter temperature to solar proton events will be discussed in Section 6.

6. Discussion

It has been said that we cannot give a general interpretation of our theoretical source spectra behavior on the sole basis of the relationships between the energy change rates (1)–(6) since their behavior in the events of **Figure 2** is different from that in **Figure 3** and both differ from that in **Figure 4**, implying that the kind of processes, their sequence of occurrence and their importance is not the same from event to event To interpret this behavior we cannot remit ourselves to the amount of traversed material, positing that particles originated in the invisible side of the sun or in the eastern hemisphere have lost more energy, because in that case events as such as the March 30, 1969 or February 2, 1969 ones would behave like the events of **Table 1**. Moreover, our hypothesis does not consider deceleration of particles after acceleration, while they traverse the solar atmosphere. Therefore, we believe that the explanation is on the basis of the parameter temperature: that is, we argue that solar proton flares develop under three main different temperature regimes, a low one that we shall denominate *cold* events ($T \approx 10^3$–$10^{5\circ}$K) (**Table 3**), an intermediate regime that we shall call *warm* events (≈10^5–l$0^{7\circ}$K) (**Table 4**), and a high temperature regime that we shall call hereafter *hot* events (T > 107°K) (**Table 3**). On the basis of this conjecture, let us discuss the main results of the preceding section:

Concerning points 1(a), 1(b) and 1(c), we can comment that as the medium was very hot, collisional losses were very high, making spectrum (18) better than spectrum (15); due to the high temperature and high density in the source nuclear reactions took place and thus spectrum (23) is even closer than (18) to the experimental curve.

Furthermore, the fact that the best fit is given by (27) seems to indicate that beyond a certain temperature, the source material is able to expand and consequently particles which have not escaped the source are adiabatically cooled. In addition, since spectrum (15) is better than (31) it is assumed that compression of the medium did not take place in high temperature regions, and so neither did adiabatic heating of protons. The irregular behavior of spectrum (23) at $E \leq 30$ MeV and $E \geq 800$ MeV in the January 28, 1967 event in relation to the tendency outlined in the last section, may be interpreted as indicating that the low energy protons observed in this event did not originate in. the same process, which explains why the observations show a high flux of protons at energy lower than the threshold acceleration value for in a medium of density $n \approx 10^{13}\text{cm}^{-3}$• Therefore, these particles may form part of the high energy tail of a preliminary heating process which were not transported by the expanding material. This

would mean that only deceleration by collisional losses and p–p collisions took place during the acceleratory process. At high energies, although energy losses from p–p collisions are stronger than collisional losses (**Figure 1**), it can be speculated that the low flux of high energy protons escape very fast from the acceleration region, so that the contribution of this process at high energies was not very important during the time scale of the acceleration.

Concerning point 2 of the last section, we assume that the acceleration process in the events of **Figure 3** was carried out in a low temperature regime so that collisional losses were completely unimportant in relation to the acceleration rate, and nuclear reactions did not take place, at least within the acceleration phase. Furthermore, a compression of the local material is associated with low temperature regimes as indicated by the fact that spectrum (31) systematically gives the best fit to the experimental curves (e.g. November 12, 1960 event).

Points 3(a)–3(d) are interpreted as follows: the temperature and density associated with the acceleration region was high enough to favor nuclear reactions, but not the expansion of source material; consequently, collisional losses of low energy protons were important in the events of **Figure 4**, providing spectrum (23) with a better description of the experimental curve. Also, because the higher temperature does not allow for a compression of the material, spectrum (31) is systematically deflected in relation to spectrum (15). Furthermore, the sudden change in the order of the sequence of curves (15) (19) and (23) is the combined effect of the temperature associated to each event and the importance of the accelerated flux of high energy protons as discussed above with respect to the January 28, 1967 event; the lower the temperature the faster spectrum (19) deflects in relation to (15) (e.g. the November 15, 1960 and November 18, 1968 events); and the higher the flux of the accelerated high energy protons, the later spectrum (23) deflects in relation to (19) (e.g. the February 25, 1969 and January 24, 1971 events).

Related to point 3(e) of last section, it would appeal that the temperature associated with this event was not very high, so that collisional losses were significant only on the low energy protons. Because of the low flux of the accelerated protons in this event, the effect of *p–p* collisions diminishes as energy increases. This event behaves almost like the cold events of **Figure 3**, since energy losses are negligible in relation to the acceleration rate of high energy protons. The reason why beyond 2 GeV spectrum (19) is more deflected than (27) is that the latter includes the *p–p* contribution to this event and collisional losses are unimportant on high energy particles (**Figure 1**). Interpretation of 3(b) and 3(e) must also consider the fact that high energy particles escape faster from the acceleration volume, and so, they are subject to energy degradation by *p–p* collisions during the acceleration time.

The interpretation of 4(a) follows from the fact that in cold events the contribution of the adiabatic heating is translated into a lower effort of the acceleration mechanism; however, in the hot and warm events (**Tables 1** and **3**) adiabatic heating did not occur, and so no effect was produced.

In relation to the interpretation of 4(b) to 4(d) it must be pointed out that the inverse proportionality between α and E_c follows from the fact that for a given situation the requirement for effective acceleration is lowered while the acceleration efficiency becomes progressively higher. On the other hand, the addition of energy losses to a given situation (same row in the

Tables) generally entails an increase in the requirement of energy E_c, and thus an increase of $\boldsymbol{\alpha}$ in order to exceed the new barrier. However, the irregularities synthetized in points 4(c) and 4 (d) of last section, which can be seen on **Tables 1–3**, that may be explained in the following manner: the critical energy, $\boldsymbol{E_c}$, is defined at low energies where the effect of adiabatic deceleration is negligible in relation to the other processes involved (**Figure 1**), and thus for a same value of $\boldsymbol{\alpha}$ the values of E_c from (19) and (23) are remarkably similar. Nevertheless, the decrease of the values of $\boldsymbol{\alpha}$ in column 7 of **Table 1** may be explained by the fact that although the requirement for acceleration is the same, as in column (6), a supplementary process is acting on the particles, and efficiency of the process is being lowered. Since E_c and α behave inversely, the value of $\boldsymbol{E_c}$ appears to increase; but in fact the real value of E_c in this event was ∼11.6 MeV. Besides, we see from columns 6 and 7 of **Tables 2** and **3** that under the hypothetical situation of the presence of adiabatic cooling in these events, the efficiency α appears higher in relation to that of column 6, given that there is an additional barrier to overtake. The value of $\boldsymbol{E_c}$ should behave similarly, but since the value of E_c in (13) is the same as that in (19), then, this hypothetical increase of α shown in column 7 in relation to that of column (6) implies a decrease of the value of $\boldsymbol{E_c}$ in column 7; this in fact does not occur because adiabatic cooling did not take place and thus the real values of $\boldsymbol{\alpha}$ and $\boldsymbol{E_c}$ in events of **Tables 1** and **3** were those of columns 3 and 6 respectively. The interpretation of 4 (e) follows from the definitions of Eqs. (31) and (32), whereas points 4(f) and 4 (g) cannot have a coherent interpretation, what can be attributed to the complexity and variability of conditions from flare to flare (e.g. the medium density, temperature, conductivity, magnetic field strength, magnetic topologies, etc.). In relation to point 4(h) it must be mentioned that deduce the same result by discussing three main different temperature regimes in the acceleration region of solar particles [105]; they estimate threshold values for proton acceleration of 1, 2.7 and 5.5 MeV for a cold region, an intermediate one and a hot region. These values are slightly lower than ours, since they do not take into account all the energy loss processes we·did. In any event, as we discussed previously, the threshold value E_c increases with the temperature because energy loss processes are increased with this parameter.

In addition to the suggestion of three temperature regions in acceleration regions extended by [105], several other suggestions have been presented in this direction: the author in [78] has discussed temperatures of $10^{4\circ}$K suggested by the central peak of hydrogen emission lines, up to more than $10^{8\circ}$K suggested by thermal emissions of X-rays. Furthermore, the flare phenomenon has usually been interpreted on basis of a dual character): the optical flare of $T\sim10^{4\circ}$K and high electron density, and on the other hand, the high energy flare plasma of $T\sim10^{7}$–$10^{9\circ}$K and relatively low electron density. The existence of several temperature regimes during a given flare has also been evoked by suggesting that the emitting regions have a filamentary and intermingling structure with hot filaments about 1 km. of diameter imbedded in cooler material [113, 115], or by suggesting a cooling of a hot region during the flare development [17, 135]. Some other models for explaining the flare energy output suggest several phases of the phenomenon, each associated with a different temperature; for example, a of relatively low temperature thermal phase followed by an explosive high temperature phase [13, 50–52, 111] posit similar models. We have not attempted to place our results into the framework of what of any of these interpretations of the flare phenomenon, but rather only to demonstrate that the generation of solar particles is accompanied by, several processes whose occurrence is narrowly related to, the

temperature of the medium, and to suggest that the acceleration regions must be associated alternately with the hot and cold aspects present during a flare or even in a pre-flare state, but certainly under very different temperature regimes from flare to flare.

Related with the expansion and compression of the source medium, there are some observational indications [84] which propose a minimum value of $\sim 3 \times 10^{7^\circ}$K for expansion. The author in [102, 103] has studied hydromagnetic criteria for expansion and compression of the sunspot magnetic lines, which he distinguishes as two different phases of the flare development; although he shows that sometimes the expansion phase may not present itself according to our findings such as we found in warm and cold events. However, in Sakurai's model acceleration occurs during the compression phase, whereas our results indicate that expansion of the source material may also occur during the acceleration process; moreover, our analysis does not show indications of expansion and compression during the same event during the phase of particle acceleration. Nevertheless, we see that, with exception of the November 12, 1960 event, the acceleration efficiency is very high where there is a compression (cold event), presumably due to the strong spatial variations of the of the longitudinal and transversal field lines, as suggested by [101, 102].

It must be emphasized that we have taken into account that expansion of closed structures occurs only within a height lower than ~0.6 to 1 solar radius, and thus expansions beyond this distance may be associated with propagation of shock waves generated in relation to type II burst or CME; therefore, our assumptions concern only adiabatic cooling through the local expansion of the source and not in higher the solar envelope.

In the specific case of the November 18, 1968 event, for which our results do not indicate any expansion of the source, observations reported a loop expansion; however s it is usually supported the fact that there is no mass motion but only a traveling excitation front. It must also be mentioned that it is generally accepted that low energy protons are much more likely to be subject to adiabatic cooling since high energy protons are rather dominated by drifts and scattering in field inhomogeneities [27, 33]; Moreover, according to [131, 132, 133] adiabatic deceleration disappears as the density of the accelerated particles decreases, so that when particle velocity is much higher than both the velocity of the medium and the Alfven velocity, the adiabatic cooling is null. This would imply that in the case of our hot events (**Figure 2**) protons of energy much higher than ~670 MeV should not be adiabatically cooled in a medium of $T > 10^{8^\circ}$K, however, our results show that even higher energy protons were adiabatically decelerated. Therefore, we claim that at least in these two events, our results support the hypothesis that particles were accelerated in closed magnetic field lines with high confinement efficiency.

Now turning to the problem of *p–p* nuclear collisions in some solar flares: we had mentioned that the value of $N_H \sim 10^{13}$ cm^{-3} was an average value in flare regions, since in fact concentrations as high as 10^{16} cm^{-3} have been reported (e.g. [118]) which implies that Eq. (23) and Eq. (27) will remain near the observational curves. This feature leads us to speculate that some flares have a high proton concentration medium (e.g. January 24, 1971), whereas in others the concentration is much lower (e.g. July 7, 1966), and that a great spread in high energy gamma rays and neutron fluxes is expected from flare to flare. The difference between observational and theoretical fluxes of gamma ray and neutrons is not a matter of discussion here, we only

want to note that these fluxes are mainly generated from the most energetic protons which are in fact the first to escape and do not frequently interact with the medium, as discussed previously in relation with some events of **Figures 2** and **4**. This implies that depending on the magnetic confinement efficiency in each flare, the expected flux of the secondary radiation will be of greater or lesser importance. According to **Figures 2** and **4** a high gamma ray flux must be generated in the February 25, 1969, January 24, 1971 and September 1, 1971 events, whereas a lower flux should be expected from the July 7, 1966 event and no gamma-ray fluxes from nuclear collision in the acceleration volume must be expected in the events of **Figure 3**. The variability of the expected high energy gamma-ray fluxes has been previously discussed in [25]. Concerning neutron fluxes we argue that they are strongly absorbed by a neutron capture reaction $(n + H_e^3 \rightarrow H^3 + p)$.

It must be pointed out that the need of protons for a minimum energy in order to overtake energy losses and to be accelerated upwards, measured energies may not be a strong requirement since the temporal and spatial sequence of phenomena in a flare seem to indicate the occurrence of a two-step acceleration of solar particles (e.g. [19, 16, 123]). A great variety of preliminary acceleration processes capable of accelerating particles up to some MeV has been suggested (e .g. [104, 112], etc.). It ·can be assumed that a certain portion of the low energy tail of the particle spectrum may belong to the first acceleration step. By smoothing the experimental data we have obtained a peculiar shape for this low energy tail of some spectra, although a similar shape is predicted from the theoretical point of view [5]. Moreover, authors in [94] discuss a noticeable deviation of the power spectrum below ≈ 4 MeV in low energy proton events, which they attribute to collisional losses during storage in the ionized medium of the low corona. We are aware of the difficulty of estimating the exact shape of the low energy spectrum, due to the strong modulation of these particles either within or outside of the source. Therefore, we argue that in addition to energy losses, this particular slope change in the low energy tail of some spectra may be due to an upper cutoff in the preliminary acceleration process.

Now let us discuss the assumption made in Section 5 in taking τ as a constant value: although it is expected that the mean confinement time varies according to particle rigidity, it is not clear if the escape mechanism from the source occurs through leakage, by thin or thick scattering, by curvature drifts, by gradient drifts or even by a sudden catastrophic disruption of a closed magnetic structure at the source; therefore, we opted for a mean value τ = 1 sec. Whose implications can be seen as follows: we note from Eq. (11) that if the value of τ increases, then $J(>E)$ increases, whereas if τ decreases, then $J(>E)$ decreases and so the theoretical spectra will approximate the experimental curves. At any rate, what can be deduced is that if τ is either lower or higher than the assumed value, the sequence of theoretical spectra does not change or consequently our conclusions are not altered. In order to evidence that the value of τ is in general of the order assumed, we shall develop the following considerations: if we make the extreme assumption that acceleration of solar protons is performed by a low efficiency process, such as a second-order Fermi-type mechanism then we know that in these cases the acceleration efficiency is given as $\alpha = V_a^2/v\iota$, where v is the velocity of protons, ι the acceleration step within the acceleration volume, and V_a the hydromagnetic velocity of the magnetic field irregularities. Taking into account that our values of α in a given event can be considered as

an average value for different energies of protons, we shall estimate the average value of ι for a 50 MeV proton and assume that the value of ι is typical of the acceleration region configuration; hence for a field strength of 500 G and density $n = 10^{13}$ cm^{-3}, the extreme values of α obtained are α = 0.1 and 1.54 s^{-1} leading to the following values: ι =10 Km and 0.84 Km respectively, which are of the same order as the values found by Perez-Peraza (1975) for multi-GeV solar protons. To estimate τ in a magnetic field (H) where the field gradient is ≈H/ι, we use the fact that $\tau = L^2/v\iota$, where L is the linear size of the acceleration region; an approximate' value of L may be deduced by the fact that the volume of flare regions varies from 10^{25} to 10^{29}cm^3 from flare to flare [19, 54, 55], and hence a linear dimension of $\sim 10^9$ cm may be considered as a typical value [30, 31] Assuming that the acceleration volume cannot be greater, than the flare volume, we shall consider $L = 10^8$ cm as a typical linear dimension for acceleration regions [116]. In such conditions we obtain τ = 1 and 12.6 s. for solar events where $\boldsymbol{\alpha}$**=** 0.13 and 1.54 s^{-1} respectively. We should say that if a shorter length scale L than the assumed one were taken values of τ <1 could be obtained, and hence our theoretical fluxes *J (>E)* would come closer to experimental curve as discussed above. In fact, it can be observed in **Figure 3**, that the theoretical curve corresponding to $\boldsymbol{\alpha}$=0.13 and thus to a low value of τ (the November 12, 1960 event) is nearer the experimental curve than to the theoretical curve corresponding to higher values of α, where it is supposed that τ must be higher. It must be noted that a higher value of α in one event with respect to another event does not imply a shorter escape time for particles in the former with respect to the latter, because the source conditions are not the same from one event to the other, as can be seen from the fact that magnetic inhomogeneities are much closer between them in events of high acceleration efficiency. We have considered a second-order Fermi-type mechanism to illustrate that even in the extreme case of such low efficiency the acceleration process may be performed within the flare time scale and to show that the assumption of τ = 1 s is well justified. If instead of a second-order Fermi mechanism we consider a first-order Fermi-type process in a shock wave, such as is usually attributed to the acceleration of solar particles (e.g. [32, 110]) the resulting value of τ is then lower than 1 s. From the study of heavy nuclei overabundances in solar cosmic rays it can be predicted that the value of τ is comprised between 0.1 and 0.4 s; these values when included in our calculations result in a much better fit of the theoretical spectra to the observational curves that the one illustrated with τ = 1 s.

The acceleration time scale of protons in solar flares, can be estimated from the following expression: $t = \int_{E_c}^{E} \frac{dE}{f(E)}$. In the energy range $10^6 \lesssim E \lesssim 10^{10}$ eV we have according our results discussed in last section that,

$$f(E) = \begin{cases} \alpha\beta W \\ (\alpha\beta + \rho\beta^2)W \end{cases} \text{ in low temperature regimens}$$

$$f(E) = \left(d - hE^{-2} - jE^{-1}\right)\beta W - b/\beta \text{ in intermediate temperature regions}$$

$$f(E) = \left[\left(d - hE^{-2} - jE^{-1}\right)\beta - \rho^2\right]W - b/\beta \text{ in high temperature regimens}$$

(where) $d = \alpha - f - \eta$

Therefore, a consideration of the parameters obtained α and E_c for a medium density $n = 10^{13}$ cm^{-3} give acceleration times much lower than the time scale of the explosive phase of the flare phenomenon. For instance, for a low efficiency event ($\alpha = 0.14$) in a high temperature regime, the time necessary to accelerate a proton from 10 MeV to 5000 MeV, is only of the order of 8 sec.

It is interesting to comment on the estimated parameter ι on the basis of our results of the parameter α: as pointed out by [102] the time scale of the explosive phase in solar flares, is $\sim 10^3 s$, and it is believed to be that of the stored magnetic energy dissipation, which is given as

$$\tau_d = 4\pi\sigma l^2/c^2 \tag{35}$$

where l is the characteristic length of the system and σ the electrical conductivity in flare material is of the order of 2.1×10^{12}–2.4×10^{14} s^{-1}. A single calculation with (35) shows us that $l = 1.7 \times 10^4$–1.8×10^5 cm which agrees well with the values estimated in this work and previously deduced by [79].

It worth comment on the discrepancy between the predicted theoretical energy spectra at the source and the experimental spectra measured in the earth environment: first we note that the physical processes that can occur in a medium as dense as the sun's atmosphere are undoubtedly very diverse, and so, we do not claim to have included in our treatment all loss processes for charged particles, but only those of greatest interest that can affect protons within the energy range we are concerned with and during the short time scale of the acceleration durability. In fact, although Cerenkov losses are included in Eq. (2) we have ignored other losses from collective effects, however, some of them, such as energy 10 s by plasma perturbations see to be negligible for protons o f $E > 23$ MeV; also we have not considered energy losses caused by viscosity and Joule dissipation as suggested by [120]. On the other hand, we have not included nuclear transformation within the acceleration volume, as for instance proton production by neutron capture, nor loss of particles from the accelerated flux as leakage from the acceleration volume. Therefore, it is expected that the consideration of these neglected processes, together with a lower value of τ as discussed above and a higher proton concentration of the medium would depress our theoretical fluxes in greater congruency with the experimental curves. Again, local modulation of particles at the source level after acceleration are not examined here, either by an energy degradation step in a closed magnetic structure, or while traversing the dense medium of the solar atmosphere as studied by [121].

In fact, observations of low energy particles indicate the existence of a strong modulation within a small envelope of $\sim$ 0.2–0.3 A.U. (e.g. [34]). Furthermore, studies of relativistic solar flare particles during the May 4,.1960 and November 18, 1968 events have shown that particles diffuse in the solar envelope (< 30 R_s) [9, 21, 22, 63] which entails a modulation of the solar fluxes. Evidences of partic1e storage in the sun, where particles can be strongly decelerated, have been widely mentioned in the literature (e.g. [1, 65, 106]). Modulation in interplanetary space is a complicated process (e.g. [28, 29]) which provokes both the depression in the number density of particles and their strong deceleration: estimations of [74] indicate that particles lose $\sim$ 10–64% of their energy through propagation, while [75, 76] sustains a loss of

$\sim$ a half of their energy before escaping into interstellar space. Moreover, the acceleration of particles in interplanetary space [21, 22, 85] may strongly disturb the spectrum. Given the strong modulation of solar particles at different levels, one cannot expect a good fit between the predicted source spectrum and the experimental one. Nevertheless, we believe that the kind of intercomparison performed here permits the clarification of ideas about the processes related to the generation of solar flare particles.

7. Concluding remarks

In order to provide some answers to the numerous questions associated with the generation of solar particles (e.g. [24, 26, 71, 102, 119]) we have attempted to study the physical processes and physical conditions prevailing in solar cosmic ray sources by separating source level effects from interplanetary and solar atmospheric effects. On this basis, we have drawn some inferences from the intercomparison of the predicted theoretical energy spectra of protons in the acceleration region with the experimental spectra of multi-GeV proton events. Concerning this kind of events a number of modern techniques have been recently developed (e.g. [72]) and the, the PGI group in Apatity, Mursmansk, Russia [124–128]. In some of GLE it has been frequent to discern two particles populations: a prompt component and a delayed one. A new kind of classification has been proposed, *GLE's* and *SubGLE*'s depending the number of station that register the earth level enhancement, location and latitude of NM stations.

We have chosen to study this particular kind of solar events (GLE) because they allow the study of the behavior of local modulation on protons, through the widest range of solar particle energies. Although one should expect that local modulation by particle energy losses at the source should follow the behavior illustrated in **Figure 1**, our results on source energy spectra indicate that is not the general case, but local modulation varies from event to event, depending on the particular phenomena that take place at the source according to the particular physical parameters prevailing in each event, such as density, temperature, magnetic field strength as well as the acceleration efficiency and particle remaining time before they escape from the source.

In drawing conclusions about the physical processes at the source, we have assumed a fixed value of the parameter n, taking into account that although spectroscopic measurements show a variation in the value of n from flare to flare, these fluctuations are nonetheless very near the value $n = 10^{13}$ cm^{-3} [115], and thus our conclusions about energy loss processes in the acceleration region are not significantly altered by small fluctuation on this parameter. Moreover, an analysis of the electromagnetic emission associated with flares indicate a spread of several decades on the medium temperature in flare regions ($\sim 10^4$–$10^{8\circ} K$), hence we have chosen to fix the parameter n in order to concentrate our analysis on the parameter temperature. On the other hand, in drawing conclusions about the physical parameter of the acceleration process we have selected a mechanism with an energy gain rate proportional to particle energy as is the case of stochastic acceleration by MHD turbulence [36]; nevertheless, we believe that our results can in general be considered as valid, in the sense that whatever the

acceleration mechanism may be, the physical conditions of the medium (density, temperature, field strength) state undoubtedly state the kind of phenomena occurring at the source. We have shown that even a low efficient mechanism (low values of α) is able to explain the generation process within the observation time scale of the explosive phase of flares, when severe conditions in the density of the medium are assumed.

Finally, let us discuss the global conception of the generation process of solar particles, according to the results obtained in this work: it is first assumed that in association with the development of solar flare conditions for the acceleration of particles may be such that it can take place either in a hot medium or in a cold one; in the first case, as a result of some powerful heating process, the local plasma must be strongly heated and acceleration of particles up to some few MeV must take place. This preliminary heating must follow to a some specific kind of hydromagnetic instability or a magnetic field annihilation process in a magnetic neutral current sheet, so that by means of electron-ion and electron-neutral collisions, Joule dissipation, viscosity, slow and fast Alfven modes or even acoustic and gravity waves, the local plasma attain very high temperature $\geq 107^{\circ}$K. The processes involved in this preliminary process of particle acceleration is not yet completely well understood; several plausible processes capable to accelerate particles up to some MeV have been suggested in the literature (e.g. [112]). Among many possibilities suggested, we believe that the one proposed by [108] presents a very plausible picture: a very select group of fast particles appearing from the preliminary heating can be reaccelerated up to very high energies, probably by a Fermi-type mechanism as proposed by [108]. Because the medium is very hot and dense we propose that collisional and *p–p* nuclear collisions between the fast protons and particles of the medium take place. Besides, we predict that up to some definite temperature the kinetic pressure of the gas is such that it favors the hydromagnetic expansion of a closed field line configuration, and thus adiabatic deceleration of particles takes place during their acceleration in the expanding plasma. Those particles with very low energy with respect a threshold energy E_c (determined by the competition between the acceleration and the deceleration rates) cannot escape from the sunspot magnetic field configuration because of their low rigidity, and thus, by scattering with the atoms, ions and electrons of the turbulent plasma, their energy is rapidly converted into heat to rise the local plasma temperature while the selected particles go into the main acceleration process. As noted by [110] the increase of electron temperature tends to decrease the efficiency of acceleration, such as that obtained in the case of *hot* events (**Table 1**) with regard to the events of **Tables 2** and **3**. This low efficiency is also related to the relatively large characteristic length- scale of the magnetic field, so that the acceleration time of particles up to high energies is relatively long. A second kind of solar event may be distinguished from the previous one, when the temperature is not so high (*warm* events in **Table 3** and **Figure 4**) and thus expansion of the source material does not take place, at least during the time of the particle acceleration process. The temperature being lower and the characteristic magnetic field length shorter than in hot events, the acceleration efficiency is higher and consequently the acce1eration time is relatively shorter. In these events or in *hot* events a low flux of high energy gamma rays generated by nuclear collisions of highly energetic protons is expected, because these fast particles spend very short time in the source before they escape. On the other hand, conditions in solar flares may be such that energy losses of protons are negligible during the acceleration process, because particles are generated by a very efficient process in a shorter acceleration time. This kind of events are assumed to occur when the acceleration region is associated

with a relatively cold plasma, such that below a certain critical temperature, a compression of the sunspot field lines takes place and thus particles are more efficiently accelerated because the characteristic magnetic field length scale is reduced. Moreover, adiabatic heating of protons into the compressed plasma may occur within the short acceleration time of these events raising the net energy exchange rate. Since the energy loss rate is negligible by rapport to the energy gain rate in these events, particles may practically be accelerated regardless of their energies, so that a preferential acceleration of heavy nuclei as suggested by [48, 49], must be expected when acceleration occurs in a region of low temperature regime. Either by assuming that in *cold* events particles are picked up from a thermal plasma or that in *warm* and *hot* events the preliminary heating is of quasi-thermal nature, a very small fraction ($N_0 \sim 10^{-11}$-10^{-18}) of plasma particle of the source volume need to be picked up by the acceleration process in order to explain the experimental spectra.

The most important parameters concerning the source and acceleration process of solar particles deduced under the assumptions made in in this work may be summarized as follows: acceleration efficiency $\alpha = 0.1 - 1.5\ s^{-1}$, characteristic magnetic field length in the acceleration volume $\iota = 3 \times 10^4$–10^6 cm, linear dimension of the acceleration volume $L = 10^9$ cm, field strength of magnetic field inhomogeneities ~500 G, hydromagnetic velocity $Va = 3.5 \times 10^7$cm s^{-1}, medium density $n \sim 10^{13}$ cm^{-3}, mean confinement time of particles within the acceleration volume $\tau \sim 0.1$–4 s, average acceleration time of individual protons $t = 12$ s, medium temperature $T \sim 10^4$–$10^{8\circ}$K. Finally, we add that whatever the approach may be in developing flare models, an expansion and compression of the source material (e.g. [96]) local modulation of particles after the acceleration processes and a plausible absorption of secondary radiation from nuclear collisions in the solar environment must be considered.

Epilogue

We would like to emphasize that this work is to some extent with the aim to pay homage to the forefathers-founders of solar cosmic ray physics and space physics.

Acknowledgements

We are very grateful to the B.S. **Alejandro Sánchez Hertz** for his valuable help in the preparation of the figures.

A. Appendix

Energy spectrum of energetic particles accelerated in a plasma by a stochastic type-Fermi acceleration process ($\sim \alpha\beta W$) while losing energy simultaneously by collisional losses according to the general expression of [10], operative throughout all the range from suprathermal to ultrarelativistic energies, given in Eq. (2.1) in Section II. In this case, the equation to be solved when only collisional losses are competing with acceleration is

$$\frac{dW}{dt} = \alpha\beta W - \frac{k}{\beta} ln\left(k_1\beta^2\right)\left[R_4 H(\chi_e) + R_5 H\left(\chi_p\right)\right] \qquad \left(\frac{MeV}{seg}\right) \tag{A.1}$$

where all the factors appearing in (A1) were defined below Eq. (2.1) in Section II

Now we proceed to a variable change, in terms of $\gamma = \frac{1}{\left(1-\beta^2\right)^{\frac{1}{2}}}$ since $W = Mc^2\gamma$, $dW = Mc^2 d\gamma$ and

$$\beta = \frac{\sqrt{\gamma^2 - 1}}{\gamma} \tag{A.2}$$

Hence

$$\alpha\beta W = \alpha\frac{\sqrt{\gamma^2 - 1}}{\gamma} Mc^2\gamma = Mc^2\alpha\sqrt{\gamma^2 - 1} \tag{A.3}$$

Therefore, Ec. (A.1) as a function of γ can be rewritten in the following form

$$\frac{d\gamma}{dt} = \alpha\sqrt{\gamma^2 - 1} - \frac{\kappa}{Mc^2}\frac{\gamma}{\sqrt{\gamma^2 - 1}} \ln\left(\frac{\kappa_1\left(\gamma^2 - 1\right)}{\gamma^2}\right)\left[R_4 H(x_e) + R_5 H\left(x_p\right)\right] \tag{A.4}$$

From where

$$dt = \frac{d\gamma}{\alpha\sqrt{\gamma^2 - 1} - \frac{\kappa}{\mu c^2}\frac{\gamma}{\sqrt{\gamma^2 - 1}} \ln\left(\frac{\kappa_1(\gamma^2 - 1)}{\gamma^2}\right)\left[R_4 H(x_e) + R_5 H\left(x_p\right)\right]} \tag{A.5}$$

and thus

$$t = \frac{1}{\sqrt{b^2 - 4ac}}\left[ln\left|\frac{2a\left(\sqrt{\gamma^2 - 1}/\gamma\right) + b - \sqrt{b^2 - 4ac}}{2a\left(\sqrt{\gamma^2 - 1}/\gamma\right) + b + \sqrt{b^2 - 4ac}}\right|\left|\frac{2a\left(\sqrt{\gamma_c^2 - 1}/\gamma_c\right) + b - \sqrt{b^2 - 4ac}}{2a\left(\sqrt{\gamma_c^2 - 1}/\gamma_c\right) + b + \sqrt{b^2 - 4ac}}\right|\right] \tag{A.6}$$

For integration of (A.5) we have assumed the case when $b^2 > 4ac$

$$\text{(were) } a = -\alpha; b = -f'\left(\gamma_T\right); c = \alpha - f\left(\gamma_T\right) + \frac{\sqrt{\gamma_T^2}}{\gamma_T} f'\left(\gamma_T\right);$$

$$f(\gamma) = \frac{1}{\gamma^3 - \gamma}\frac{\kappa}{mc^2} ln\left(\frac{k_1\left(\gamma^2 - 1\right)}{\gamma^2}\right)\left[R_4 H(x_e) + R_5 H\left(x_p\right)\right] \text{ (and)}$$

$$f'(\gamma) = \frac{\kappa}{Mc^2}\frac{\left[R_4 H(x_e) + R_5 H\left(x_p\right)\right]}{\sqrt{\gamma^2 - 1}}\left[\left(-3 - \frac{2}{\gamma^2 - 1}\right) ln\left(\frac{k_1\left(\gamma^2 - 1\right)}{\gamma^2}\right) + \frac{2}{\gamma^2 - 1}\right]$$

$$+ \frac{\kappa}{Mc^2}\frac{1}{\gamma(\gamma^2 - 1)} ln\left(\frac{k_1\left(\gamma^2 - 1\right)}{\gamma^2}\right)\left\{R_4 R_2 e^{-x_e^2}\left[1 - c_4\left(1 - 2x_e^2\right)\right] + R_5 R_3 e^{-x_p^2}\left[1 - c_5\left(1 - 2x_p^2\right)\right]\right\}$$

Now, according to Eq. (8.1) in Section IV the differential spectrum in terms of γ is,

$$N(\gamma)d\gamma = \frac{N_0}{\tau Mc^2} e^{-t/\tau} dt \tag{A.7}$$

And from (A.6) we obtain

$$e^{-t/\tau} = \left[\left|\frac{2a\left(\sqrt{\gamma^2-1}/\gamma\right)+b-\sqrt{b^2-4ac}}{2a\left(\sqrt{\gamma^2-1}/\gamma\right)+b+\sqrt{b^2-4ac}}\right|\left|\frac{2a\left(\sqrt{\gamma_c^2-1}/\gamma_c\right)+b-\sqrt{b^2-4ac}}{2a\left(\sqrt{\gamma_c^2-1}/\gamma_c\right)+b+\sqrt{b^2-4ac}}\right|\right]^{\frac{1}{\tau\sqrt{b^2-4ac}}} \tag{A.8}$$

in such a way that Eq. (A.7) can be rewritten

$$N(\gamma)d\gamma = \frac{N_0}{\tau Mc^2} \frac{\left[\left|\frac{2a\left(\sqrt{\gamma^2-1}/\gamma\right)+b-\sqrt{b^2-4ac}}{2a\left(\sqrt{\gamma^2-1}/\gamma\right)+b+\sqrt{b^2-4ac}}\right|\left|\frac{2a\left(\sqrt{\gamma_c^2-1}/\gamma_c\right)+b-\sqrt{b^2-4ac}}{2a\left(\sqrt{\gamma_c^2-1}/\gamma_c\right)+b+\sqrt{b^2-4ac}}\right|\right]^{\frac{1}{\tau\sqrt{b^2-4ac}}} d\gamma}{\alpha\sqrt{\gamma^2-1} - \frac{\kappa}{\mu c^2}\frac{\gamma}{\sqrt{\gamma^2-1}}\ln\left(\frac{\kappa_1(\gamma^2-1)}{\gamma^2}\right)\left[R_4H(x_e)+R_5H(x_p)\right]} \tag{A.9}$$

which is the differential spectrum as a function of gamma.

To obtain the integral spectrum we resort to Eq. (9) of Section IV,

$$J(>\gamma) = \int_{\gamma}^{\gamma_m} N(\gamma)d\gamma = \frac{N_0}{Mc^2} e^{t(\gamma_c)/\tau}\left[e^{-t(\gamma)/\tau} - e^{-t(\gamma_m)/\tau}\right] \tag{A.10}$$

Introducing A.8 in A.10 we obtain the integral spectrum

$$J(>\gamma) = \frac{N_0}{Mc^2}\left|\frac{2a\left(\sqrt{\gamma_c^2-1}/\gamma_c\right)+b-\sqrt{b^2-4ac}}{2a\left(\sqrt{\gamma_c^2-1}/\gamma_c\right)+b+\sqrt{b^2-4ac}}\right|^{1/\tau\sqrt{b^2-4ac}} \left[\left|\frac{2a\left(\sqrt{\gamma^2-1}/\gamma\right)+b-\sqrt{b^2-4ac}}{2a\left(\sqrt{\gamma^2-1}/\gamma\right)+b+\sqrt{b^2-4ac}}\right|^{1/\tau\sqrt{b^2-4ac}} - \left|\frac{2a\left(\sqrt{\gamma_M^2-1}/\gamma_M\right)+b-\sqrt{b^2-4ac}}{2a\left(\sqrt{\gamma_M^2-1}/\gamma_M\right)+b+\sqrt{b^2-4ac}}\right|^{1/\tau\sqrt{b^2-4ac}}\right] \tag{A.11}$$

Eqs. A.9 and A.12 may become very important for the study of all the entire range of particle energy of solar particles, particularly low energy protons measured by satellites in the interplanetary space, that presumably they have been affected in their sources. Eventually this approach could be used at laboratory scale for experiments of particle energization in plasmas.

Author details

Jorge Perez-Peraza* and Juan C. Márquez-Adame

*Address all correspondence to: perperaz@geofisica.unam.mx

Instituto de Geofisica, Universidad Nacional Autonoma de Mexico, D.F. for CDMX, Mexico

References

[1] Alhualia. 12th ICRC, Tasmania, Hobart; 1971. p. 468

[2] Bai T, Ramaty R. Solar Physics. 1976;**49**:343

[3] Barcus JG. Solar Physics. 1969;**8**:186

[4] Bazilevskaya GA, Charakhchyan AN, Charakhchyan TN, Lozutin IL. 12th I.C.R.C., Tasmania. 1971;**5**:1825

[5] Biswas S, Radhakiskshnan B. Solar Physics. 1973;**28**:211

[6] Bland. Nuovo Cimento. 1966;**13**:427

[7] Bruzek A. Solar Physics. 1972;**26**:94

[8] Bukata RP, Gronstal PI, Palmeira RAR, McCracken KG, Rao UR. Solar Physics. 1969;**10**:198

[9] Burlaga. Solar Physics. 1970;**13**:348

[10] Buttler ST, Buckingham MJ. Physical Review. 1962;**126**:1

[11] Bryant DA, Cline TL, Desai VD, McDonald FB. Astrophysical Journal. 1965;**141**:478

[12] Cameron AGW. The Astrophysical Journal Letters. 1967;**1**:35

[13] Cheng C-C. Solar Physics. 1972;**22**:178-188

[14] Chupp EL. Space Science Reviews. 1971;**12**:486

[15] Chupp EL, Forrest DJ, Higbie PR, Suri AN, Tsai C, Dunphy PP. Nature. 1974;**241**:333

[16] Cline T. NASA-X-661-7133, GSFC, Greenbelt, Maryland;1970

[17] Datlowe D. Solar Physics. 1971;**17**:436

[18] Davis L. In: Mackin RJ, Neugebauer M, editors. The Solar Wind. NY: Pergamon Press; 1966

[19] De Jager C. Solar Physics. 1967;**2**:327

[20] Dessai UD. Canadian Journal of Physics. 1971;**49**:265

[21] Duggal SP, Guidi I, Pomerantz MA. Solar Physics. 1971;**18**:234

[22] Duggal SP. Reviews of geophysics. Space Physics. 1979;**17**:1021

[23] Dulk GA, Altschuler MD, Smerd SF. Astrophysical Journal Letters. 1971;**8**:235

[24] Elliot H. In: Wilson JG. Progress in Cosmic Ray Physics, Vol. 1;1952

[25] Elliot H. Planetary and Space Science. 1964;**12**:657

[26] Elliot H. In: De Jager C, Svestka Z, editors. N Solar Flares and Space Research. Amsterdam: North Holand Pub; 1969. p.356

[27] Elliot H. In: De Jager C, editor. Solar-Terrestrial Physics, Part I; 1972. p.134

[28] Englade RC. 12th International Conference on Cosmic Rays. 1971;**2**:502

[29] Englade RC. Journal of Geophysical Research. 1972;**77**:6266

[30] Ellison MA, McKena SMP, Reid. Dunsink Observatory Publications. 1961. 53

[31] Ellison MA, Reid JA. Research in Geophys. 1964 M.I.T. Presstime 1,43

[32] Fichtel CE, McDonald FB. Annual Review of Astronomy and Astrophysics. 1967;**5**:359

[33] Fisk LA, Axford WI. Journal of Geophysical Research. 1968:73. DOI: 10.1029/JA073i013 p04396 ISSN 0148-0227

[34] Fisk LA. 14th ICRC; Munich. 1975;**2**:810

[35] Fritzova-Svestkova, Svetska. Solar Physics. 1967;**2**:87

[36] Gallegos-Cruz A, Pérez-Peraza J. Astrophysical Journal. 1995;**446**:669

[37] Ginzburg VL, Syrovatskii SI. The Origin of Cosmic Rays. Oxford: Pergamon Press;1964

[38] Ginzburg VL. Elementary Processes for Cosmic Ray. Astrophys, Gordon & Breach;1969

[39] Heristchi Dj, Kangas J, Kremser G, Legrand JP, Masse P, Palous M, Pfotzer G, Riedler W, Whilhem K. Annals of the International Quiet Year. 1967;**3**:267

[40] Heristchi Dj, Trottet G. Physical Review Letters. 1971;**26**:197

[41] Heristchi DJ, Perez-Peraza J, Trottet G. In: Lincoln V, editor. Bulletin of the World Data Center A, Upper Atmosphere Geophysics, Boulder Colorado. Vol. **24**; 1972. 182

[42] Heristchi Dj, Perez-Peraza J, Trottet G. Paper SP-5.3-9 14th ICRC. 1975;**5**:1841

[43] Heristchi Dj, Trottet G, Perez-Peraza J. Solar Physics. 1976;**49**:141

[44] Hess WN. Reviews of Modern Physics. 1958;**30**:368

[45] Ifedili SO. Solar Physics. 1974**39**:233

[46] Jokipii JR. Reviews of Geophysics and Space Physics. 1971;**9**:1

[47] King JH. J. Spacecraft Rockets. 1974;**11**:40l

[48] Korchak AA, Sirovatskii SI. Soviet Doklady. 1958;**3**:983

[49] Korchak AA, Sirovatskii SI. Proc of the 6th ICRC 3, 216. Moscow: Izd AN SSSR (in Russian); 1960

[50] Korchak AA. Astronomicheskii Zhurnal. 1967a;**11**:258

[51] Korchak AA. Doklady AN SSSR. 1967b;**12**:192

[52] Korchak AA, Platov YV. Astronomicheskii Zhurnal. 1968;**45**(6):1185

[53] Krimigis SM. Journal of Geophysical Research. 1965:70, 2943

[54] Krivsky. Acta Physica Academiae Scientiarum Hungaricae. 1970;**29**:427

[55] Krivsky L. Nuovo Cimento Series. 1965;**10-27**:1017

[56] Kurochka LN. Astronomicheskii Zhurnal. 1970;**47**:111

[57] Lin RP. Journal of Geophysical Research. 1968;**73**:3066

[58] Lin RP, Kahler SW, Roelof EC. Solar Physics. 1960;**4**:338

[59] Lingelfelter RE, Ramaty R. In: Shen BSP, editor. High Energy Nuclear Reactions in Astrophysics. New York: Benjamin WA, Inc; 1967. p. 99

[60] Lockwood JA. Journal of Geophysical Research. 1967;**72**:3395

[61] Lockwood JA. Journal of Geophysical Research. 1968;**73**:4247

[62] Lockwood JA, Webber WR, Hsieh L. Journal of Geophysical Research. 1974;**79**:4149

[63] Lust R, Simson JA. Physical Review. 1957;**108**:1563

[64] McCracken KG. 1969 in Solar Flares and Space Research, Ed. by De Jager, C. and Svetska, Z. North Holland Pub, Amsterdam, p. 202

[65] McDonald FB, Dessai. Journal of Geophysical Research. 1971;**76**:808

[66] Malville JM, Smith SF. Journal of Geophysical Research. 1963;**68**:3181

[67] Miroshnichenko L, Sorokin MO. Geomagn and Aeronomy. 1985;**25**(4):534

[68] Miroshnichenko LI, Sorokin MO. Geomagnetism and Aeronomy. 1986;**26**(4):535

[69] Mirosnichenko LI, Pérez-Peraza J. Astrophysical Aspects in the studies of solar cosmic rays. International Journal of Modern Physics. 2008;**23**:1

[70] Mirosnichenko LI, Vashenyuk EV, Pérez-Peraza J. Bulletin of the Russian Academy of Sciences. 2009;**73**(3):297

[71] Miroshnichenko L. Solar cosmic rays: Fundamental and applications. Astrophysics and Space Science Library. 2015;**405**

[72] Mishev AL, Kocharov LG, Usoskin G. J.G.R.: Space Physics. 2014;**119**:670

[73] Ogilvie KW, Bryant DA, Davis LR. Journal of Geophysical Research. 1962;**67**(3):929

[74] Palmer IA. Reviews of Geophysics and Space Physics. 1982;**20**:335

[75] Parker EN. Interplanetary Dynamical Processes. New York: John Wiley & Sons, Interscience;1963a

[76] Parker EN. ApJ. 1963b. Suppl 77;**8**:177

[77] Parker. Planetary and Space Science. 1965;**13**(1):9

[78] Parker EN. Space Science Reviews. 1969;**9**:325

[79] Perez-Peraza J. Journal of Geophysical Research. 1975;**80**:3535

[80] Perez-Peraza J, Galindo Trejo J. Revista Mexicana De Astronomia Y Astrofisica. 1975;**1**:273

[81] Perez-Peraza J, Gallegos-Cruz A. The Astrophysical Jornal Supplements. 1994a;**669**:90-92

[82] Perez-Peraza J, Gallegos-Cruz A. Geofísica Internacional. 1994b;**33-2**:311

[83] Pinter S. Solar Physics. 1969;**8**:149

[84] Pinter S. Proc. IV Leningrad Cosmic Phys. Seminar, Phys. Techn. Inst., Leningrad; 1972p.63

[85] Pomerantz, Duggal. Journal of Geophysical Research. 1974;**79**:913

[86] Ramaty R, Lingelfetter RE. High Energy Phenomenon on the sun NASA SP-342; 1973. 301

[87] Ramaty R, Lingelfelter RE. Journal of Geophysical Research. 1967;**72**:879

[88] Ramaty R, Stone RG. High Energy Phenomenon on the Sun NASA SP-342;1973. 341

[89] Ramaty R, Lingelfetter RE. In: Kane RS, editor. N Solar Gamma, X and EUV Radiation, IAU Symposium 68. Dordrecht, Holland: Reidel Pub Co; 1975. p. 363

[90] Ramudarai S, Biswas S. 12th International Cosmic Rays Conference. Vol. 21971. p. 793

[91] Ramudarai S, Biswas S. Astrophysics and Space Science. 1974;**30**:187

[92] Reames DF, Fichtel CE. 10th ICRC, CAL. 1967;**2**:546

[93] Reid JH. Dunsink Obs. Publ.1961;53

[94] Rotwell PL. Journal of Geophysical Research. 1976;**81**:709

[95] Sakurai K. Journal of Geomagnetism and Geoelectricity. 1963;**14**:144

[96] Sakurai K. Publications of the Astronomical Society of Japan. 1965;**19**:408

[97] Sakurai K. Publications of the Astronomical Society of Japan. 1966a;**18**:77

[98] Sakurai K. Report of Ionosphere and Space Research in Japan 20 519. 1966b;**20**:233

[99] Sakurai K. Report of Ionosphere and Space Research in Japan 21. 1967;**21**:113, 213

[100] Sakurai K. NASA Report X- 693-71-268 GSFC, Greenbelt Md1971

[101] Sakurai K. Solar Physics. 1973;**31**:483

[102] Sakurai K. Physics of Solar Cosmic Rays. Tokio, Japan: University of Tokyo Press; 1974

[103] Sakurai K. Publications of the Astronomical Society of Japan. 1976;**28**:177

[104] Schatzman E. Solar Physics. 1967;**1**:411

[105] Severnii, Shabanskii. Soviet Astronomy - Astrophysical Journal. 1961;**4**:583

[106] Simnet. Solar Physics. 1971;**20**:448

[107] Smerd SF, Dulk GA. Solar Magnetic Fields, IAU 431971. p. 616

[108] Smith EVP. In: Oman Y, editor. N Mass Motions in Solar Flares and Related Phenomena, Nobel Symposium 9. Stockholm: Almqvistand Wiksell; 1968. p. 137

[109] Smith SF, Ramsay HE. Solar Physics. 1967;**2**:158

[110] Smith DF. Advances in Space Research. 1986;**6**(6):135

[111] Somov BV, Syrovatskii SI. Solar Physics. 1974;**39**:415

[112] Sonnerup. In: Ramaty R, Stone RG, editors. High Energy Phenomena on the Sun, NASA X-693-73-193. 1973. p. 357

[113] Suemoto, Hiei. Publications of the Astronomical Society of Japan. 1959;**11**:185

[114] Suemoto, Hiei. Publications of the Astronomical Society of Japan. 1962;**14**:33

[115] Svestka Z. BAC. 1963;**14**:234

[116] Svetska Z. Bulletin of the Astronomical Institute of Czechoslovakia. 1966;**17**:262

[117] Svetska Z. Solar Physics. 1968;**4**(1):18

[118] Svetska, Z. 1969 in Solar Flares and Space Research (ed. By de Jager, C. and Svestka, Z.) North-Holland Pub., Amsterdam, p. 16.

[119] Svetska Z. Solar Flares Geophysical and Astrophysics Monographs. Dordrecht Holland: Reidel Publishing Company; 1976

[120] Syrovatskii SI. Soviet Physics - Journal of Experimental and Theoretical Physics. 1961;**13**: 1257

[121] Syrovatskii SI, Shmelevae OP. Soviet Astronomy - Astrophysical Journal. 1972;**16**:273

[122] Takakura T. Space Science Reviews. 1966;**5**:80

[123] Takakura T. Solar Physics. 1969;**6**:133

[124] Vashenyuk EV, Balabin YV, Perez-Peraza J, Gallegos-Cruz A, Miroshnichenko LI. Advances in Space Research. 2006;**38**(3):411

[125] Vashenyuk EV, Balabin YV, Miroshnichenko LI, Pérez-Peraza J, Gallegos-Cruz A. 30th Int. Cosmic Ray, Mérida. Vol. 12007a. p. 249

[126] Vashenyuk EV, Miroshnichenko LI, Balabin Y-V, Pérez-Peraza J, Gallegos-Cruz A. 30th Int. Cosmic Ray Conf., Merida. 2007b;**1**:253

[127] Vashenyuk EV, Balabin YV, Miroshnichenko LI. Advances in Space Research. 2008;**41**(6):926

[128] Vashenuyk EV. Bulletin of the Russian Academy of Sciences. 2011;**75**(6):767

[129] Vernov SN, Grigorov NL, Zatespin GT, Chudakov AE. Izvstia Akademii Nauk Sssr, Deriya Series Fizika (English Translation). 1955;**19**:45

[130] Webber WR. In: Hess WW, editor. AAS-NASA SP-50 Symp. On the physics of Solar flares, GSFC. 1964. p. 515

[131] Wentzel DG. Journal of Geophysical Research. 1965;**70**:2716

[132] Wentzel DG. ApJ. 1969a;**156**:303

[133] Wentzel DG. ApJ. 1969b;**157**:545

[134] West HI Jr, Buck RM, Walton JR, D'Arcy RG Jr. Upper Atmosph. Geophys World Data Center A, NOAA, Rep. 241972. p. 113

[135] Widding KG. IAU Symposium. 1975;**68**:153

[136] Wild JP. Journal of the Physical Society of Japan. 1962;**17**(Suppl. A II):249

IntechOpen